Award Number: W81XWH-12-1-0389

TITLE: Connexins and Cadherin Crosstalk in the Pathogenesis of Prostate Cancer

PRINCIPAL INVESTIGATOR: Parmender P. Mehta

CONTRACTING ORGANIZATION: University of Nebraska
Omaha, NE 68198

REPORT DATE: September 2015

TYPE OF REPORT: Annual

PREPARED FOR: U.S. Army Medical Research and Materiel Command
Fort Detrick, Maryland 21702-5012

DISTRIBUTION STATEMENT: Approved for Public Release;
Distribution Unlimited

The views, opinions and/or findings contained in this report are those of the author(s) and should not be construed as an official Department of the Army position, policy or decision unless so designated by other documentation.

REPORT DOCUMENTATION PAGE

Form Approved
OMB No. 0704-0188

Public reporting burden for this collection of information is estimated to average 1 hour per response, including the time for reviewing instructions, searching existing data sources, gathering and maintaining the data needed, and completing and reviewing this collection of information. Send comments regarding this burden estimate or any other aspect of this collection of information, including suggestions for reducing this burden to Department of Defense, Washington Headquarters Services, Directorate for Information Operations and Reports (0704-0188), 1215 Jefferson Davis Highway, Suite 1204, Arlington, VA 22202-4302. Respondents should be aware that notwithstanding any other provision of law, no person shall be subject to any penalty for failing to comply with a collection of information if it does not display a currently valid OMB control number. **PLEASE DO NOT RETURN YOUR FORM TO THE ABOVE ADDRESS.**

1. REPORT DATE	2. REPORT TYPE	3. DATES COVERED
September 2015	Annual	1 Sep 2014 - 31 Aug 2015

4. TITLE AND SUBTITLE

Connexins and Cadherin Crosstalk in the Pathogenesis of Prostate Cancer

5a. CONTRACT NUMBER

5b. GRANT NUMBER
W81XWH-12-1-0389

5c. PROGRAM ELEMENT NUMBER

6. AUTHOR(S)
Parmender P. Mehta

5d. PROJECT NUMBER

5e. TASK NUMBER

5f. WORK UNIT NUMBER

7. PERFORMING ORGANIZATION NAME(S) AND ADDRESS(ES)
University of Nebraska
Lincoln, NE 68588

8. PERFORMING ORGANIZATION REPORT NUMBER

9. SPONSORING / MONITORING AGENCY NAME(S) AND ADDRESS(ES)
U.S. Army Medical Research and Materiel Command
Fort Detrick, Maryland 21702-5012

10. SPONSOR/MONITOR'S ACRONYM(S)

11. SPONSOR/MONITOR'S REPORT NUMBER(S)

12. DISTRIBUTION / AVAILABILITY STATEMENT
Approved for Public Release; Distribution Unlimited

13. SUPPLEMENTARY NOTES

14. ABSTRACT

Gap junctions (GJ) are conglomerations of cell-cell channels that are formed by a family of 21 distinct proteins, called connexin (Cx)s. The Cxs are transmembrane proteins, which are designated according to molecular mass. They are assembled into GJs through many steps (Figure 1A). Communication through GJs is crucial for maintaining homeostasis [1;2]. Impaired, or loss of, Cx expression has been documented in the pathogenesis of various carcinomas [1;3-5]. Moreover, many studies have shown that over-expression of Cxs in tumor cells attenuates the malignant phenotype in vivo and in vitro, reverses the changes associated with epithelial to mesenchymal transformation (EMT), and induces differentiation [3;4;6]. For example, Cx32 is expressed in the liver, lung, and exocrine glands, and knock out studies have shown that the incidence of carcinogen-induced tumors in these mice is higher [7-9]. Moreover, mutations in several Cx genes have been characterized in inherited diseases associated with aberrant proliferation and differentiation [1;10]. These studies support the notion that Cxs act as tumor suppressors. Despite this the molecular mechanisms by which Cxs are assembled into GJs and how GJs are disassembled are poorly understood.

15. SUBJECT TERMS- none provided

16. SECURITY CLASSIFICATION OF:			17. LIMITATION OF ABSTRACT	18. NUMBER OF PAGES	19a. NAME OF RESPONSIBLE PERSON
a. REPORT	b. ABSTRACT	c. THIS PAGE			USAMRMC
U	U	U	UU		19b. TELEPHONE NUMBER *(include area code)*

Parmender P. Mehta, Ph.D.

Table of Contents

Parmender P. Mehta, Ph.D.

1. Introduction:

Gap junctions (**GJs**) are conglomerations of cell-cell channels that are formed by a family of 21 distinct proteins, called connexin **(Cx)**s. The Cxs are transmembrane proteins, which are designated according to molecular mass. They are assembled into GJs through many steps (**Figure 1**). Communication through GJs is crucial for maintaining homeostasis [1;2]. Impaired, or loss of, Cx expression has been documented in the pathogenesis of various carcinomas [1;3-5]. Moreover, many studies have shown that over-expression of Cxs in tumor cells attenuates the malignant phenotype *in vivo* and *in vitro*, reverses the changes associated with epithelial to mesenchymal transformation (**EMT**), and induces differentiation [3;4;6]. For example, Cx32 is expressed in the liver, lung, and exocrine glands, and knock out studies have shown that the incidence of carcinogen-induced tumors in these mice is higher [7-9]. Moreover, mutations in several Cx genes have been characterized in inherited diseases associated with aberrant proliferation and differentiation [1;10]. These studies support the notion that Cxs act as tumor suppressors. Despite this the molecular mechanisms by which Cxs are assembled into GJs and how GJs are disassembled are poorly understood.

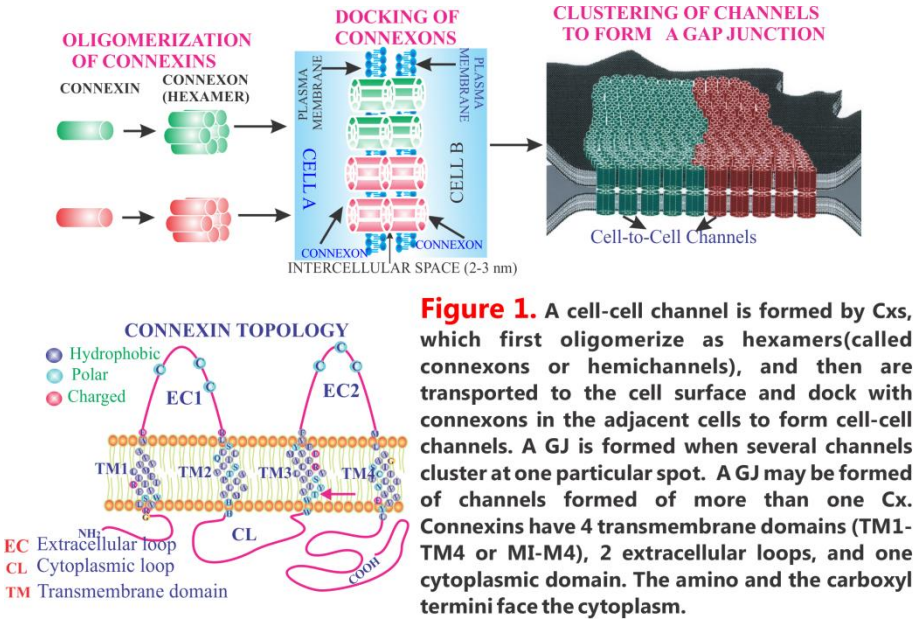

Figure 1. **A cell-cell channel is formed by Cxs, which first oligomerize as hexamers(called connexons or hemichannels), and then are transported to the cell surface and dock with connexons in the adjacent cells to form cell-cell channels. A GJ is formed when several channels cluster at one particular spot. A GJ may be formed of channels formed of more than one Cx. Connexins have 4 transmembrane domains (TM1-TM4 or MI-M4), 2 extracellular loops, and one cytoplasmic domain. The amino and the carboxyl termini face the cytoplasm.**

2. Body

Our central hypothesis is that bidirectional signaling between cadherin(Cad)s and Cxs is required to maintain the polarized and differentiated state of epithelial cells and that GJ assembly is the downstream target of the signaling initiated by the classical Cads, with epithelial (E)-cad facilitating assembly and neuronal (N)-cad disrupting the assembly. We had proposed 2 specific aims to test this hypothesis:

1. **Determine how E-cad mediated cell-cell adhesion controls the assembly of Cxs into gap junctions in human prostate cancer (PC) cell lines.**

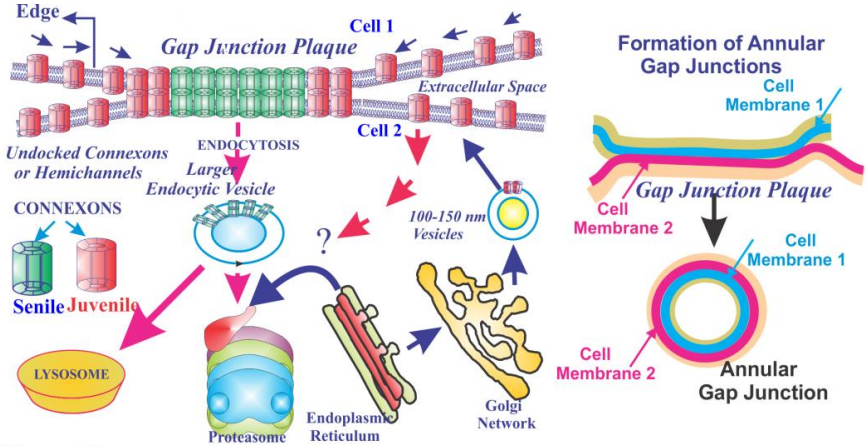

Figure 2. **Assembly and Disassembly of GJs. Cxs are short lived proteins with a half life of 2-5 h. Connexons (see Figure 1) traffic to the plasma membrane (PM) in 100-150 nm particles, diffuse laterally and dock with their counterpart connexons in the PM of apposed cells. Juvenile connexons (red) are recruited to the periphery of the GJ plaque while senile connexons (green) are pinched off from the middle as double membrane vesicles into either one or the other cell. Alternatively, an entire GJ plaque is also endocytosed in its entirety into one or the other cell called annular GJs(left).**

2. Determine the molecular mechanisms by which E-cad and N-cad modulate gap junction assembly differentially in human prostate cancer cell lines.

It is as yet unknown how a bi-cellular structure, such as a GJ, also called a GJ plaque, is endocytosed [1;10-12]. Connexins are short-lived proteins and both the assembly of Cxs into GJs and their disassembly are multi-step processes, which are poorly understood (**Figures 1 & 2**). A GJ can be endocytosed into one or the other cell, either in its entirety, also called an annular GJ, or as fragments pinched off from the center of the plaque as double membrane vesicles, by endocytosis and targeted to the lysosome for degradation. Alternatively, undocked connexons may be endocytosed by clathrin mediated or non-clathrin mediated endocytosis (**Figure 2**) [13-16].

Tasks of Aim 1:

1. Prepare recombinant retroviruses that contain various E-cad constructs that alter its ability to mediate cell-cell adhesion.
    a. Prepare recombinant retrovirus containing E-cad (W156A) (**Johnson**).
    b. Prepare recombinant retrovirus containing E-cad with deleted β-catenin binding site (**Johnson**).
    c. Prepare recombinant retrovirus containing E-cad with mutated p120 catenin binding site (**Johnson**).

2. Generate stable polyclonal cultures of several human PC cell lines (LNCaP - **ATCC**; PC3 - **ATCC**; RWPE1 - **ATCC**; PZ-HPV-7 -**ATCC**) expressing the constructs shown in 1 (**Mehta**).

3. In the cells described in 2, determine if connexins are assembled into GJs using Triton X-100 solubility assays (**Mehta and Johnson**).

4. In the cells described in 2, determine if cadherins are assembled into adherens junctions using Triton X-100 solubility assays (**Mehta and Johnson**).

5. In the cells described in 2, observe the trafficking of connexins and their assembly into GJs (**Mehta and Johnson**).
    a. Perform cell surface biotinylation to detect connexins at the plasma membrane (**Mehta**).
    b. Determine if connexins co-localize with EEA1, clathrin or caveolin-1 (**Mehta and Johnson**).

6. Knock down endogenous E-cadherin in LNCaP prostate cancer cells (**ATCC**) with or without connexin expression (**Mehta**).

    a. Determine if motility is altered in cells expressing E-cadherin or connexins (**Johnson**).

7. Determine if the trafficking of connexins is altered in knock down cells described in 6 (**Mehta**).

Statement of Work

Aim 1: Determine how E-cadherin mediated cell-cell adhesion controls the assembly of connexins into gap junctions in human prostate cancer cell lines.

Parmender P. Mehta, Ph.D.

Tasks:

1) Prepare recombinant retroviruses that contain various E-cadherin constructs that alter its ability to mediate cell-cell adhesion. (Months 1-9)

- **a) Prepare recombinant retrovirus containing E-cadherinW156A (E-cad-W156A)(Johnson).**
- **b) Prepare recombinant retrovirus containing E-cadherinΔβ-catenin (E-cadΔβ-cat)(Johnson).**
- **c) Prepare recombinant retrovirus containing E-cadherinΔp120-catenin (E-cadΔp120-cat)(Johnson).**

The preparation of the constructs E-cad-W156A, E-cadherinΔβ-cat (E-cadΔβ-cat) and E-cadherinΔp120 (E-cadΔp120-cat) in retroviral vectors as well as production of recombinant viruses was described in the previous report (tasks 1a, 1b).

The recombinant virus harboring E-cadherinΔp120-catenin (E-cadΔp120-cat) has not been produced (task 1c).

2) Generate stable polyclonal cultures of several human prostate cancer cell lines (LNCaP - ATCC; PC3 - ATCC; RWPE1 - ATCC; PZ-HPV-7 -ATCC) expressing the constructs shown in 1) (Mehta). (Months 3-12).

This task was accomplished and the findings were reported in the previous report (Figures 3, 4, and 5 in 2014 progress report).

3) In the cells described in 2), determine if connexins are assembled into gap junctions using Triton X-100 solubility assays (Mehta and Johnson). (Months 4-16)

Expression of E-cad as well as α-Cat and the effect on the assembly of Cx43 into GJs in highly metastatic prostate cancer cell line, PC3-M, was described in 2014 report (**Figure 7**). E-cad remained intracellular despite robust expression. Also, Cx43 and N-cad remained detergent-soluble (**Figure 7**).

The constructs E-cadΔβ-cat and E-cadΔp120-catenin have not yet been introduced into any cell line yet.

When we retrovirally expressed α-Cat in PC-3M cells, we found that its expression inhibited growth profoundly (**Figure 3A**) and induced epithelioid morphology (**Figure 3B**) compared to those infected with the control retrovirus. As an additional control, we also expressed E-Cad in PC-3M cells and found that its expression also inhibited growth discernibly but not as robustly as α-Cat (**Figure 3A**). Immunocytochemical analyses showed that α-Cat was localized at the cell-cell contact regions (**Figure 3C, second panel**). PC-3M cells express N-Cad. Intriguingly, we found that whereas N-Cad was predominantly localized at the cell-cell contact regions (**Figure 4C, third panel)**, E-Cad was found both in the cytosol and cell-cell contact areas (**Figure 4C, bottom panel**). These data were substantiated by measuring the cell number (data not shown). To corroborate the above data, we conditionally expressed α-Cat in PC-3M cells using Tetracycline/Doxycycline-inducible Retroviral System in which the transactivator and α-Cat were in the same vector. The results showed that the inducible expression of α-Cat also inhibited growth (**Figure 4A**) and induced epithelioid morphology (**Figure 4B**). Moreover, α-Cat was robustly expressed at the areas of cell-cell contact regions within 8-12 h upon induction (**Figure 4C**).

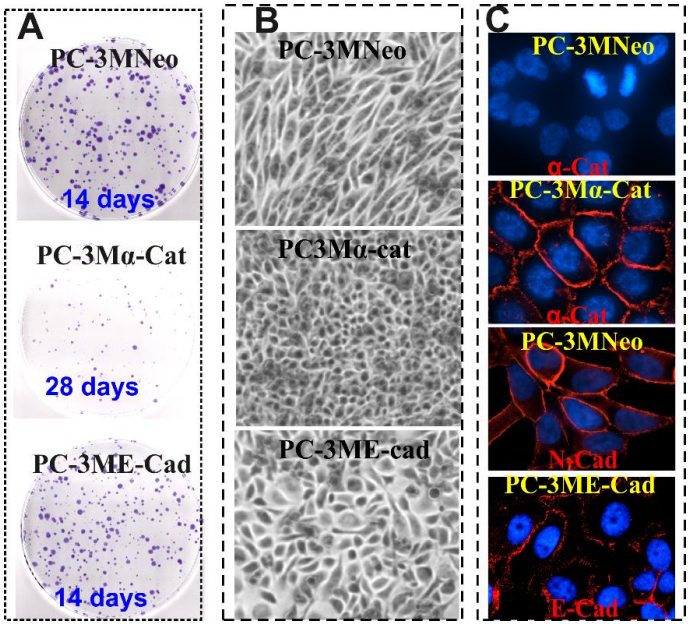

Figure 3. Expression of α-Cat inhibits growth in PC-3M cells. **A**. PC-3M cells (10,000) were multiply infected with control (PC-3MNeo), α-Cat-(PC-3Mα-Cat) and E-Cad (PC-3ME-Cad)- harboring retroviruses in 6-cm dishes & selected in G418 till sensitive cells died and dishes became confluent. Cells were trypsinized & were seeded at clonal density (1000) in G418 in replicate dishes, allowed to grow into colonies, fixed & stained with crystal violet. Note that dishes infected with α-Cat-harboring retroviruses had to be grown for 28 days to see visible colonies compared to 14 days for cells infected with the control and E-Cad-harboring retroviruses. **B**. Phase-contrast images of live cell colonies. Note a compact arrangement in PC-3M-α-Cat. **C**. Immunocytochemical localization of α-Cat in PC-3MNeo (top panel) and PC-3Mα-Cat (second panel), of N-Cad in PC-3MNeo (third panel) and E-Cad in PC-3MECad (bottom panel). Note that α-Cat (red) is not present in PC-3MNeo cells. Note also that α-Cat and N-Cad are localized at the cell-cell contact areas whereas E-Cad is also in the cytosol.

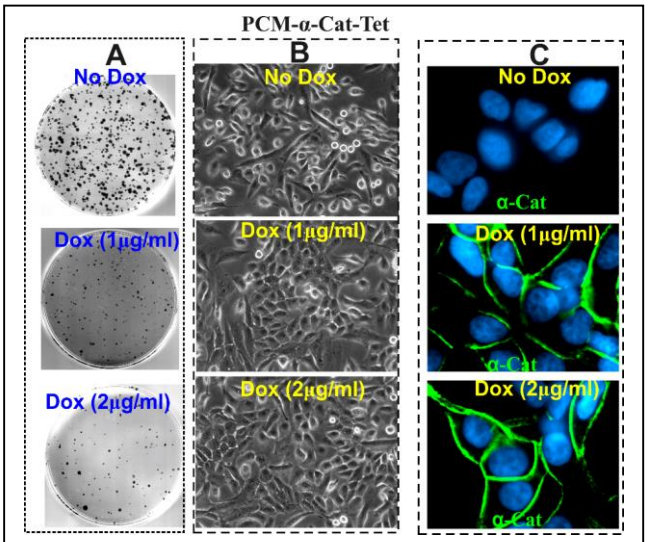

Figure 4. Inducible expression of α-Cat inhibits growth. PC-3M cells were infected with Tet-On-α-Cat retrovirus and selected as described in Figure 4 legend. These cells are named as PCM-α-Cat-Tet. **A**. Doxycycline (Dox) inhibits the growth of PCM-α-Cat-Tet cells. Cells (10^3) were seeded in the presence and absence of indicated concentrations of Dox as described in Figure 4 legend. Note reduction in the size of colonies growing in the presence of Dox. **B**. Dox alters the morphology of PCM-α-Cat-Tet cells. Note more robust cell-cell contacts and altered morphology. Cells were treated with Dox for 48 h. **C**. α-Cat (green) is robustly expressed at cell-cell contact upon Dox treatment as assessed immunocytochemically.

These findings were novel and prompted us to change the course of the proposed studies. The current experiments are aimed at understanding the molecular mechanism by which expression of α-Cat inhibits growth in PC-3M cells. .

4) In the cells described in 2), determine if cadherins are assembled into adherens junctions using Triton X-100 solubility assays (Mehta and Johnson). (Months 4-16)

The results obtained with PC3-M were described in 2014 report (**please see Figure 7**). We have not initiated these studies with other prostate cancer cell lines.

5) In the cells described in 2), observe the trafficking of connexins and their assembly into gap junctions (Mehta and Johnson). (Months 6-18)

a) Perform cell surface biotinylation to detect connexins at the plasma membrane (Mehta).
b) Determine if connexins co-localize with EEA1, clathrin or caveolin-1 (Mehta and Johnson).

The results obtained with PC3-M were described in 2014 report (please see Figures 6, 7). We have not initiated these studies with LNCaP cells and other prostate cancer cell lines.

6) Knock down endogenous E-cadherin in LNCaP prostate cancer cells (ATCC) with or without connexin expression (Mehta). (Months 12-20)

a) Determine if motility is altered in cells expressing E-cadherin or connexins (Johnson).

We have not assessed the motility of LNCaP cells after expressing E-cad–WT and E-cad-W156A. However, expression of E-cad-W156A mutant altered the morphology of LNCaP cells (**report 2014**). However, we have explored the effect of conditional expression of α-cat on the motility of PC-M cells using live-cell imaging. These results showed that α-Cat expression attenuated the motility of PC-3M cells.

7) Determine if the trafficking of connexins is altered in knock down cells described in 6) (Mehta). (Months 16-24)

We have not initiated these studies.

Aim 2: Determine the molecular mechanisms by which E-cadherin and N-cadherin modulate gap junction assembly differentially in human prostate cancer cell lines.

Tasks:

1) Prepare recombinant retroviruses that contain chimeras of E-cadherin and N-cadherin (Johnson). (Months 6-16)

a) Prepare recombinant retrovirus containing chimeras with the extracellular domains switched (Johnson).

b) Prepare recombinant retrovirus containing chimeras with the cytoplasmic domains switched (Johnson).

c) Prepare recombinant retrovirus containing chimeras with segments of the extracellular domains of E-cadherin and N-cadherin swapped (Johnson).

We have not expressed chimeras of E-cadherin and N-cadherin in LNCaP cells.

2) Infect LNCaP cells (ATCC) and PZ-HPV-7 cells (ATCC) with the retroviruses described in 1) and retroviruses containing wild-type N-cadherin (Mehta). (Months 12-24)

These results were reported in 2013 and 2014 reports

3) **In the cells described in 2), determine if connexins are assembled into gap junctions using Triton X-100 solubility assays (Mehta and Johnson). (Months 16-28)**

We have not initiated these studies.

4) In the cells described in 2), determine if cadherins are assembled into adherens junctions using

Triton X-100 solubility assays (Mehta and Johnson). (Months 16-28)

We have not initiated these studies.

5) In the cells described in 2), observe the trafficking of connexins and their assembly into gap junctions. (Months 24-32)

a) Perform cell surface biotinylation to detect connexins at the plasma membrane (Mehta).

b) Determine if connexins co-localize with EEA1, clathrin or caveolin-1 (Mehta and Johnson).

We have not initiated this task.

6) Determine if N-cadherin alters the motility of connexin-expressing LNCaP (ATCC) and cells PZ-HPV-7 (ATCC) cells (Johnson). (Months 28-36)

These results were described in 2014 report.

7) Determine if N-cadherin induces endocytosis of gap junctions in connexin-expressing LNCaP (ATCC) and PZ-HPV-7 (ATCC) cells (Mehta). (Months 28-36)

We have not initiated these studies yet.

Conclusion:

The available data preclude us to draw any conclusions with respect to the proposed studies.

Miscellaneous: While pursuing the proposed studies, we observed that the trafficking and assembly of both Cx43 and Cx32 into gap junctions are governed by the palmitoylation of specific cysteine residues in the cytoplasmic tails.

Connexin43 and Connexin32 are Palmitoylated: Based on the findings that many of the desmosomal proteins are palmitoylated (Roberts *et al.*, 2014), we rationalized that palmitoylation might regulate the assembly of Cxs into GJs. We used acyl-biotin exchange (ABE) method to detect plamitoylation (Wan *et al.*, 2007). These studies showed that Cx43 and Cx32 were palmitoylated both in the brain and several cell lines (**Figure 5**). These results prompted us to examine the role of palmitoylation in the assembly of Cx43 and Cx32 into GJs.

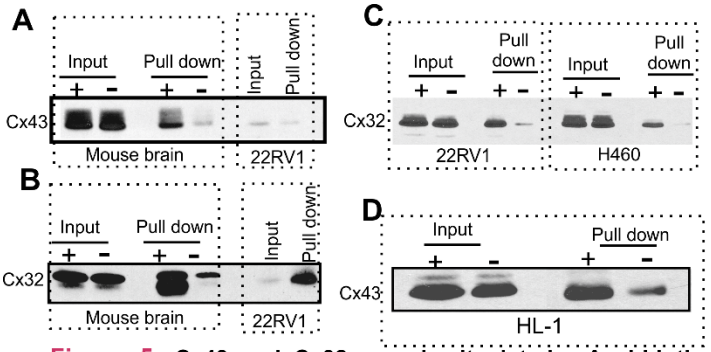

Figure 5: Cx43 and Cx32 are plamitoylated. Acyl-biotin exchange (ABE) reaction was performed with lysates from mouse brain and cultured cell lines. In ABE, palmitates in Cxs are exchaneg with biotin in the presence of hydroxylamine (+) but not in its absence (-). Cxs with exchanged biotins are pulled down with streptavidin beads and blotted with Cx-specific antibodies. A. Cx43 is plamitoylated in mouse brain as well as in human prostate cancer cell line 22RV1. B. Cx32 is plamitoylated in mouse brain and in 22 RV1cell line. Astrocytes and oligodendrocytes in mouse brain, respectively, express Cx43 and Cx32 abundantly. C. Cx32 is palmitoylated in 22RV1 (PC Cell Line) and lung cancer cell line H460. D. Cx43 is palmintoylated in rat heart cell line HL-1.

Palmitoylation Regulates the Assembly of Cx43 and Cx32 into Gap Junctions: Because the six highly-conserved cysteine(C)s in the two extracellular

loops of Cxs are disulfide-bonded and are unlikely to be palmitoylated (**Figure 1**)(Laird, 2006), we searched for other cysteines in the cytoplasmic tail of Cx43 and Cx32 as potential palmitoylation targets. We found that the three cysteines (C260, C271 and C298) in the cytoplasmic tail of Cx43, and three cysteines (C217, C260 and C263) in the cytoplasmic tail of Cx32 (shown in **Figure 1)**, could be potentially palmitoylated. To test whether plamitoylation of these cysteines has any effect on GJ assembly, we created mutants of Cx43 and Cx32 in which all the above cysteines were mutated to serines. We used rat Cx43 and Cx32. These mutants are named as Cx43-3CS and Cx32-3CS. Both wild-type Cx43 (Cx43-WT) and the mutant Cx43-3CS were retrovirally expressed in a pancreatic cancer cell line, Capan-1, from which the endogenous human Cx43 had been stably knocked down (Johnson *et al.*, 2013). Our earlier studies had shown that in Capan-1 cells the endogenously expressed Cx43 was not assembled into GJs due to its endocytosis upon arrival at the cell surface (Johnson *et al.*, 2013). The results showed that, when expressed, knocked-in rat Cx43-WT, like its endogenous counterpart, was not assembled into GJs whereas the mutant Cx43-3CS was (**Figure 6**). Similar results were obtained when Cx43-3CS was expressed in Cx-null human prostate cancer cell line, LNCaP (data not shown). Moreover, transient expression of Cx32-3CS also showed that compared to Cx32-WT, the mutant was assembled into larger GJs.

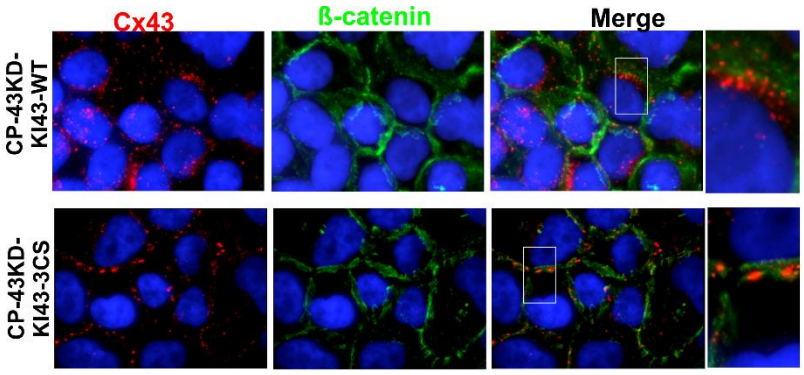

Figure 6: **Cx43-WT and Cx43-3CS were retrovirally expressed in Capan (CP)-1 cells from which endogenous Cx43 had been knocked down. Note that the knocked-in Cx43-WT ((CP-43KD-KI43-WT;red) remains scattered as intracellular puncta (top row) whereas Cx43-3CS (CP-43KD-KI43-CS, red) is assembled into discrete gap junction like puncta at the cell-cell contact areas (bottom row). Cell-cell contact was delineated by immunostaining with β-catenin (green) staining. The boxed areas are enlarged (right).**

The two major conclusions drawn from our preliminary studies are that both Cx43 and Cx32 are palmitoylated in tissues as well as in cell lines and that palmitoylation of their cytoplasmic domains inhibits their assembly into GJs.

Key Research Accomplishments

1. We have found that expression of a cell-cell adhesion deficient mutant of E-cadherin, in which tryptophan at position 156 in the first extracellular domain is replaced with alanine, acts in a dominant-negative manner when expressed in E-cadherin-expressing human prostate cancer cell line, LNCaP, and abolishes cell-cell adhesion as well as alters their morphology.
2. Expression of α-catenin in metastatic prostate cancer cell line, PC3M, in which this gene is deleted and in which connexins are not assembled into GJs, inhibits growth and partially restores GJ assembly. These findings highlight the importance of connexins and cadherins in the pathogenesis of prostate cancer.

Reportable Outcomes:

The following manuscript was published. Katoch,P., Mitra,S., Ray,A., Kelsey,L.S., Roberts,B., Wahl III JK,

Johnson KR, and Mehta,P.P. (2015). The Carboxyl Tail of Connexin32 Regulates Gap Junction Assembly in Human Prostate and Pancreatic Cancer Cells. J Biol Chem *290*, 4647-4662

The manuscript file is appended.

Appendices:

One manuscript is appended.

Supporting Data

None.

Reference List

1. Laird,D.W. (2006) Life cycle of connexins in health and disease. *Biochem J*, **394**, 527-543.
2. Saez,J.C., Berthoud,V.M., Branes,M.C., artinez,A.D., Bey., and Beyer,E.C. (2003) Plasma membrane channels formed by connexins: their regulation and functions. *Physiol Rev*, **83**, 1359-1400.
3. Crespin,S., Defamie,N., Cronier,L., and Mesnil,M. (2009) Connexins and carcinogenesis. In Harris,A. and Locke,D. (eds.) *Connexinss: A Guide*., pp 529-42.
4. Naus,C.C. and Laird,D.W. (2010) Implications and challenges of connexin connections to cancer. *Nat Rev Cancer*, **10**, 435-441.
5. Plante,I., Stewart,M.K.G., Barr,K., Allan,A.L., and Laird,D.W. (2010) Cx43 suppresses mammary tumor metastasis to the lung in a Cx43 mutant mouse model of human disease. *Oncogene*, **30**, 1681-1692.
6. McLachlan,E., Shao,Q., Wang,H.l., Langlois,S., and Laird,D.W. (2006) Connexisn act as tumor suppressors in three dimensional mammary cell organoids by regulating differentiation and angiogenesis. *Cancer Res*, **66**, 9886-9894.
7. King TJ, Gurley KE, Prunty J, Shin JL, Kemp CJ, and Lampe PD (2005) Deficiency in the gap junction protein connexin32 alters p27Kip1 tumor suppression and MAPK activation in a tissue-specific manner. *Oncogene*, **24**, 1718-1726.
8. King,T.J. and Lampe,P.D. (2004) Mice deficient for the gap junction protein Connexin32 exhibit increased radiation-induced tumorigenesis associated with elevated mitogen-activated protein kinase (p44/Erk1, p42/Erk2) activation. *Carcinogenesis*, **25**, 669-680.
9. King,T.J. and Bertram,J.S. (2005) Connexins as targets for cancer chemoprevention and chemotherapy. *Biochimica et Biophysica Acta (BBA) - Biomembranes*, **1719**, 146-160.
10. Laird,D.W. (2010) The gap junction proteome and its relationship to disease. *Trends Cell Biol*, **20**, 92-101.
11. Berthoud VM, Minogue PJ, Laing JG, and Beyer EC (2004) Pathways for degradation of connexins and gap junctions. *Cardiovasc.Res.*, **62**, 256-267.
12. Musil,L.S. (2009) Biogenesis and degradation of gap junctions. In Harris,A. and Locke,D. (eds.) *Connexins: A Guide*. Springer, pp 225-40.
13. Falk,M.M., Baker,S.M., Gumpert,A., Segretain,D., and Buckheit,R.W. (2009) Gap junction turnover is achieved by the internalization of small endocytic double-membrane vesicles. *Mol Biol Cell*, **20**, 3342-3352.
14. Jordan,K., Chodock,R., Hand,A., and Laird,D.W. (2001) The origin of annular junctions: a mechanism of gap junction internalization. *J Cell Sci*, **114**, 763-773.
15. Piehl,M., Lehmann,C., Gumpert,A., Denizot,J.P., Segretain,D., and Falk,M.M. (2007) Internalization of Large Double-Membrane Intercellular Vesicles by a Clathrin-dependent Endocytic Process. *Mol.Biol.Cell*, **18**, 337-347.
16. Traub,L.M. (2009) Tickets to ride: selecting cargo for clathrin-regulated internalization. *Nat Rev Mol Cell Biol*, **10**, 583-596.
17. Igawa,T., Lin FF, Lee MS, Karan D, Batra SK, and Lin MF (2002) Establishment and characterization of androgen-independent human prostate cancer LNCaP cell model. *Prostate*, **50**, 222-235.
18. Lin MF, Meng TC, Rao PS, Chang C, Schonthal AH, and Lin FF (1998) Expression of human prostatic acid phosphatase correlates with androgen-stimulated cell proliferation in prostate cancer cell lines. *J Biol Chem.*, **273**, 5939-5947.
19. Meng TC, Lee MS, and Lin MF (2000) Interaction between protein tyrosine phosphatase and protein tyrosine kinase is involved in androgen-promoted growth of human prostate cancer cells. *Oncogene*, **19**,

2664-2677.

20. Meng TC and Lin MF (1998) Tyrosine phosphorylation of c-ErbB-2 is regulated by the cellular form of prostatic acid phosphatase in human prostate cancer cells. *J Biol Chem.*, **273**, 22096-22104.
21. Govindarajan,R., Song,X.-H., Guo,R.-J., Wheelock,M.J., Johnson,K.R., and Mehta,P.P. (2002) Impaired traffcking of connexins in androgen-independent human prostate cancer cell lines and its mitigation by a-catenin. *J Biol Chem*, **277**, 50087-50097.
22. Mehta,P.P., Perez-Stable,C., Nadji,M., Mian,M., Asotra,K., and Roos,B. (1999) Suppression of human prostate cancer cell growth by forced expression of connexin genes. *Dev Genetics*, **24**, 91-110.
23. Mitra,S., Annamalai,L., Chakraborty,S., Johnson,K., Song,X., Batra,S.K., and Mehta,P.P. (2006) Androgen-regulated Formation and Degradation of Gap Junctions in Androgen-responsive Human Prostate Cancer Cells. *Mol Biol Cell*, **17**, 5400-5416.
24. Pettaway CA, Pathak S, Greene G, Ramirez,E., Wilson,M., Killion,J., and Fidler,I. (1996) Selection of highly metastatic variants of different human prostatic carcinomas using orthotopic implantation in nude mice. *Clin Cancer Res*, **2**, 1627-1636.
25. Ewing CM, Ru N, Morton RA, Robinson JC, Wheelock,M.J., Johnson KR, Barrett JC, and Isaacs WB (1995) Chromosome 5 suppresses tumorigenicity of PC3 prostate cancer cells: correlation with re-expression of a-catenin and restoration of E-cadherin function. *Cancer Res*, **55**, 4813-4817.
26. Nieman,M., Prudoff,R., Johnson,K., and Wheelock,M. (1999) N-cadherin promotes motility in human breast cancer cells regardless of their E-cadherin expression. *J Cell Biol*, **147**, 631-643.
27. Kim JB, Islam S, Kim YJ, Prudoff RS, Sass KM, Wheelock MJ, and Johnson KR (2000) N-Cadherin extracellular repeat 4 mediates epithelial to mesenchymal transition and increased motility. *J Cell Biol*, **151**, 1193-1206.

THE JOURNAL OF BIOLOGICAL CHEMISTRY VOL. 290, NO. 8, pp. 4647–4662, February 20, 2015
© 2015 by The American Society for Biochemistry and Molecular Biology, Inc. Published in the U.S.A.

The Carboxyl Tail of Connexin32 Regulates Gap Junction Assembly in Human Prostate and Pancreatic Cancer Cells*[S]

Received for publication, June 16, 2014, and in revised form, December 23, 2014 Published, JBC Papers in Press, December 30, 2014, DOI 10.1074/jbc.M114.586057

Parul Katoch, Shalini Mitra, Anuttoma Ray, Linda Kelsey, Brett J. Roberts, James K. Wahl III, Keith R. Johnson, and Parmender P. Mehta[1]

From the Department of Biochemistry and Molecular Biology, Department of Oral Biology, Eppley Institute for Research in Cancer and Allied Diseases, Fred and Pamela Buffett Cancer Center, University of Nebraska Medical Center, Omaha, Nebraska 68198

Background: Cytoplasmic tails of connexins are highly divergent yet their role in gap junction assembly remains undefined.
Results: Gap junctions of tail-deleted connexin32 remain small and fail to grow.
Conclusion: The cytoplasmic tail of connexin32 is dispensable for gap junction formation but essential for regulating junction size.
Significance: The cytoplasmic tails of connexins may enhance function of gap junctions by regulating their size.

Connexins, the constituent proteins of gap junctions, are transmembrane proteins. A connexin (Cx) traverses the membrane four times and has one intracellular and two extracellular loops with the amino and carboxyl termini facing the cytoplasm. The transmembrane and the extracellular loop domains are highly conserved among different Cxs, whereas the carboxyl termini, often called the cytoplasmic tails, are highly divergent. We have explored the role of the cytoplasmic tail of Cx32, a Cx expressed in polarized and differentiated cells, in regulating gap junction assembly. Our results demonstrate that compared with the full-length Cx32, the cytoplasmic tail-deleted Cx32 is assembled into small gap junctions in human pancreatic and prostatic cancer cells. Our results further document that the expression of the full-length Cx32 in cells, which express the tail-deleted Cx32, increases the size of gap junctions, whereas the expression of the tail-deleted Cx32 in cells, which express the full-length Cx32, has the opposite effect. Moreover, we show that the tail is required for the clustering of cell-cell channels and that in cells expressing the tail-deleted Cx32, the expression of cell surface-targeted cytoplasmic tail alone is sufficient to enhance the size of gap junctions. Our live-cell imaging data further demonstrate that gap junctions formed of the tail-deleted Cx32 are highly mobile compared with those formed of full-length Cx32. Our results suggest that the cytoplasmic tail of Cx32 is not required to initiate the assembly of gap junctions but for their subsequent growth and stability. Our findings suggest that the cytoplasmic tail of Cx32 may be involved in regulating the permeability of gap junctions by regulating their size.

Gap junctions are ensembles of cell-cell channels through which molecules up to 1 kDa can directly pass between the cytoplasmic interiors of adjoining cells (1, 2). Cell-cell channels are formed of Cxs,[2] which are encoded by a family of 21 distinct genes in humans and are designated according to the molecular mass. Some members of the Cx family are expressed in a tissue-specific manner, whereas the expression of others is redundant (2). Knock out studies of Cx genes have unveiled diverse roles of cell-cell communication in maintaining tissue homeostasis (3). Their roles have been substantiated by human genetic diseases, such as occulodental digital dysplasia, palmoplantar keratoderma, and keratitis-ichthyosis-deafness syndrome, in which mutations in Cx genes have been detected (3, 4). Despite tissue-specific expression of some Cxs, gap junctions in all tissues appear as disc-shaped structures consisting of several regularly spaced particles in freeze-fracture replicas (5). To form a cell-cell channel, six Cxs first oligomerize into a hexamer, called a connexon, which is transported to the cell surface and docks with a connexon in an adjacent cell. A gap junction is formed when several such cell-cell channels cluster (1). Thus, a key step in the assembly of gap junctions is the aggregation of cell-cell channels at one particular spot at areas of cell-cell contact, a process that has not yet been elaborated (6).

A Cx is a transmembrane protein that traverses the membrane four times and has one intracellular and two extracellular loops with the amino and carboxyl termini facing the cytoplasm. The transmembrane and the extracellular loop domains are highly conserved among different Cxs, whereas the carboxyl termini, often called the cytoplasmic tails, are highly divergent (2, 6). The role of the two extracellular loop domains of Cxs in the formation of cell-to-cell channels as well as of the cytoplasmic tails in regulating the opening and closing of cell-cell channels has been well documented (5, 7–9). The cytoplasmic tails of many Cxs have also been shown to interact directly or indirectly with several proteins (10). Although these interactions have been postulated to control the assembly of Cxs into gap junctions, the molecular mechanisms involved have remained unexplored (10). In particular, it is not clear what the exact role of a Cx cytoplasmic tail is and at which step it is involved in

* This work was supported, in whole or in part, by National Institutes of Health Grant R0-1DE12308 (to K. R. J.). This work was also supported by Department of Defense Prostate Cancer Research Program Grants PC-081198 and PC-111867 and Nebraska State Grant LB506 (to P. P. M.).
[S] This article contains supplemental Movies S1 and S2.
[1] To whom correspondence should be addressed: Dept. of Biochemistry and Molecular Biology, Fred and Pamela Buffett Cancer Center, University of Nebraska Medical Center, Omaha, NE 68198. Tel.: 402-559-3826; Fax: 402-559-6650; E-mail: pmehta@unmc.edu.

[2] The abbreviations used are: Cx, connexin; TX100, Triton X-100; FRAP, fluorescence recovery after photobleaching; EGFP, enhanced GFP.

Downloaded from http://www.jbc.org/ at University of NE Medical Center on December 30, 2015

regulating the assembly of gap junctions. For example, the interaction of a scaffolding protein, ZO-1, which binds to the PDZ- binding domain of several Cxs, facilitates the assembly of Cx43, an ubiquitously expressed Cx, into gap junctions (11, 12) yet has an opposite effect on the assembly of Cx50, which is expressed in lens epithelial cells (10, 13). Thus, it is highly likely that besides ZO-1, other proteins documented to interact with Cxs might inhibit or enhance gap junction assembly and disassembly in a tissue-specific and cell-context-dependent manner. Moreover, most studies with Cx-interacting proteins have been performed with Cx43, which is ubiquitously expressed (6), and not with Cxs whose pattern of expression is restricted to few tissues (2). Tissue-specific as well as redundant expression of some Cxs combined with the fact that most tissues and cell types express more than one Cx subtype (1, 14, 15) implies that the assembly of each Cx subtype into gap junctions is likely regulated spatiotemporally in a cell context and physiological state-dependent manner by distinct mechanisms to prevent fortuitous gap junction formation and internalization. The cytoplasmic tails of Cxs seem to be the likely targets for such type of regulation as they are the most divergent portions among different members of Cx gene family (2).

Among all the Cxs, the expression of Cx32 is observed in the well differentiated acinar cells of exocrine glands, such as prostate and pancreas (15). Our previous studies showed that the retrovirus-mediated expression of Cx32 in Cx-null, androgen-sensitive prostate cancer cell line, LNCaP, induced the formation of gap junctions, restored junctional communication, inhibited growth *in vitro*, and retarded malignancy *in vivo* (16). We further showed that androgens, the key players that govern prostate morphogenesis and oncogenesis (17), regulated the formation and degradation of gap junctions by controlling the expression level of Cx32 posttranslationally (18). In these studies we had fortuitously observed that the retrovirally expressed cytoplasmic tail-deleted Cx32 appeared to assemble into small gap junctions compared with those formed by the expression of the full-length Cx32 (18). Moreover, our previous study with cadherin-null human squamous carcinoma cells had also shown that the assembly of Cx32 into gap junctions was facilitated when cells acquired a partially polarized state and that the cytoplasmic tail of Cx32 (abbreviated as Cx32-CT) was required to initiate the formation of a gap junction plaque and/or its subsequent growth in these cells (19). These studies prompted us to explore the role of Cx32-CT in the assembly of gap junctions.

We demonstrate here that compared with the full-length Cx32, the cytoplasmic tail-deleted Cx32 is assembled into smaller gap junctions despite normal trafficking to the cell surface in human pancreatic and prostatic cancer cell lines. We also document that the expression of the full-length Cx32 in cells stably expressing the cytoplasmic tail-deleted Cx32 increases the size of gap junctions, whereas the expression of the cytoplasmic tail-deleted Cx32 in cells expressing the full-length Cx32 has the opposite effect. Moreover, our results show that the cytoplasmic tail is required for the clustering of cell-cell channels. Furthermore, we also show that in cells expressing the cytoplasmic tail-deleted Cx32, the expression of the cell surface-targeted cytoplasmic tail alone is sufficient to enhance gap junction assembly. In addition, by expressing a series of Cx32 deletion mutants with progressive truncations of the carboxyl tail, our results document that the critical motifs that determine the size of gap junctions reside between residues 230 and 250 of Cx32. Finally, our live-cell imaging data document that compared with the mobility of larger and smaller gap junctional plaques formed of full-length Cx32, the gap junction-like puncta composed of cytoplasmic tail-deleted Cx32 are highly mobile. Our findings suggest that the cytoplasmic tail is not required to initiate the assembly of Cx32 into gap junctions but for their subsequent growth and stability. These findings suggest that the cytoplasmic tail of Cx32 may be involved in regulating the permeability of gap junctions by regulating their size.

MATERIALS AND METHODS

Cell Culture—The human pancreatic cancer cell line, BxPC3 (CRL-1687), and a prostate cancer cell line, LNCaP (ATCC CRL 1740), were grown in RPMI 1640 and DMEM (Invitrogen) containing 7% fetal bovine serum (Sigma), respectively, in an atmosphere of 5% CO_2 at 37 °C. Stock cultures were maintained weekly by seeding 5×10^5 cells per 10-cm dish in 10 ml of complete culture medium with a medium change at day 3 or 4 as described (18, 20). New stocks were initiated after 10 passages. The two retroviral packaging cell lines, EcoPack and PTi67, were grown as described previously (16, 18). BxPC3 and LNCaP cells were infected with various recombinant retroviruses, and pooled polyclonal cultures from ~2000 colonies were grown and maintained in RPMI containing G418 (200 μg/ml) (see "Recombinant DNA Constructs and Retrovirus Production and Infection" below).

Antibodies and Immunostaining—Rabbit polyclonal and mouse monoclonal antibodies against Cx32 and mouse anti-β-catenin, and rabbit anti-β-actin have been described previously (18, 19, 21). We also used rabbit polyclonal antibodies raised against the carboxyl tail (Sigma; C-3470) and the cytoplasmic loop of Cx32 (Sigma, C-3595). For immunostaining 5×10^5 BxPC3 and 4×10^5 LNCaP cells were seeded on glass coverslips in 6-well clusters and allowed to grow for 3 days after which they were fixed with 2% paraformaldehyde and immunostained as described (19–21). Anti-rabbit and anti-mouse secondary antibodies conjugated with Alexa 488 or Alexa 594 (Invitrogen) were used as appropriate. After mounting immunostained cells on glass slides in SlowFade antifade medium (Invitrogen), images were acquired with a Leica DMRIE microscope (Leica Microsystems, Wetzler, Germany) equipped with a Hamamatsu ORCA-ER2 CCD camera (Hamamatsu City, Japan) using a 63× oil objective (NA 1.35). Several z-stacked images taken 0.3 μm apart were used to measure colocalization using the commercial image analysis program Volocity 6.0.3 (Improvision, Lexington, MA) as described (19, 20).

Recombinant DNA Constructs and Retrovirus Production and Infection—Construction of retroviral vectors containing wild-type rat Cx32 (Cx32-WT) and the cytoplasmic tail-deleted Cx32 (Cx32Δ220) has been described (18). Briefly, the Cx32Δ220 was engineered by a PCR-based cloning technique and cloned into the retroviral vector LXSN. The PCR amplification was with the forward primer (5′-GCCGAATTCATGA-ACTGGACAGGTC-3′) and the reverse primer containing a

Downloaded from http://www.jbc.org/ at University of NE Medical Center on December 30, 2015

premature stop codon (TGA, Amber) at amino acid position 221 (5′-CCGGAATTCTCAACGGCGGGCACAG-3′. The mutant was generated by site-directed mutagenesis using a QuikChange kit (Stratagene, La Jolla, CA) according to the manufacturer's instructions. The Cx32-CT-Myr construct (containing amino acid residues 220–283) was constructed by PCR cloning as follows. Cx32-CT was first cloned in-frame with pmTurqouise-C3 to create pmTurquoiseCx32Δ220. The entire pmTurquoiseCx32Δ220 was amplified by PCR with Nco1 and BamH1 sites added at the 3′ and 5′ ends, respectively. This Nco1 and BamH1 fragment was cloned into a modified pSPUTK vector, which added 5′ myristoylation and two Myc tags. The assembled cassette was removed and subcloned in pcDNA3.1 (+) as a HindIII and BamH1 fragment.

Myc-tagged Cx32-WT (Cx32-WT-Myc) and Cx32Δ220 (Cx32Δ220-Myc) were generated by PCR-based cloning. The coding sequence for the Myc tag was incorporated in the reverse primers for Cx32-WT and Cx32Δ220, which also contained the Xho1 site. The primers used were 5′-ACTCTAGCACTCGAGTTACAGGTCCTCTTCGGAGATCAGCTTCTGCTCGCAGGCTGAGCATCGGTC-3′ for Cx32-WT and 5′-ACTCTAGCATCTAGATTACAGGTCCTCTTCGGAGATCAGCTTCTGCTCACGGCGGGCACAGGC-3′ for Cx32Δ220. The PCR products were cloned into the EcoR1 and Xho1 site of pcDNA3.1(+) and retroviral vector pLXSN. Cx32-WT and Cx32Δ220 were fused in-frame with the enhanced green fluorescent protein using pEGFP-N1 (Clontech, Mountain View CA) to create Cx32-WT-EGFP and Cx32Δ220-EGFP, which were subcloned into retroviral vector LXSN using the standard recombinant DNA methodology described in our earlier studies (20). All constructs were verified by DNA sequencing (ACGT Inc, Wheeling, IL or at the University of Nebraska Medical Center core facility).

The retroviral vectors were used to produce recombinant retroviruses in EcoPack and PTi67 packaging cell lines as described previously (19–21). The recombinant retroviruses produced from the pooled polyclonal cultures of PTi67 cells were assayed for virus titer by colony forming units as described (22). BxPC3 and LNCaP cells were multiply (2–4 times) infected with the recombinant retroviruses and selected in G418 (400 μg/ml) for 2–3 weeks in complete medium. Pooled cultures from ~2000 colonies obtained from 3–4 dishes were expanded, frozen, and maintained in selection media containing G418 (200 μg/ml). Pooled polyclonal cultures were used within 2–4 passages for immunocytochemical and biochemical analyses.

Detergent Extraction and Western Blot Analysis—BxPC3 (3×10^6) and LNCaP (2×10^6) cells, seeded in replicate 10-cm dishes in 10 ml of complete medium, were grown for 72 h. The procedures for cell lysis, detergent-solubility assay with 1% Triton X-100 (TX100) and Western blot analysis have been described previously (18, 19, 21). Normalization was based on equal cell number for the analysis of detergent-soluble and -insoluble fractions by SDS-PAGE analysis of cell lysates.

Cell Surface Biotinylation Assay—BxPC3 (5×10^5) and LNCaP (4×10^5) cells were seeded in 6-cm dishes in replicates and grown to 70–80% confluence. A biotinylation reaction using freshly prepared EZ-LinkSulfo-NHS-SS Biotin reagent (Pierce) at 0.5 mg/ml in phosphate-buffered saline (PBS) supplemented with 1 mM $CaCl_2$ and 1 mM $MgCl_2$ (PBS-PLUS) was performed at 4 °C for 1 h. Cells were lysed after quenching the reaction with PBS-PLUS containing 20 mM glycine as described previously (19, 21, 23). The affinity precipitation of biotinylated proteins was from 200 μg of total protein using 100 μl of streptavidin-agarose beads (Pierce) on a rotator overnight at 4 °C. SDS-PAGE followed by Western blotting was used to resolve the streptavidin-bound biotinylated proteins after elution as described previously (19, 21, 23). The kinetics of degradation of cell surface-associated Cx32-WT and Cx32Δ220 was determined essentially as described previously (20, 21). The protein concentration was determined using the BCA reagent (Pierce).

Cell Transfection—Twenty-four hours before transfection, BxPC3 (1.5×10^6) and LNCaP (10^6) cells were seeded on glass coverslips in 6-well clusters. Cells were transfected with various plasmids in duplicate using XtremeGENE (Roche Diagnostics) according to the manufacturer's instructions. We found XtremeGENE to be superior for LNCaP and BxPC3 cells compared with several other lipid-based reagents that we tried. For transfections, 2 μg of plasmid DNA was used per well. For co-transfection of two plasmids, pmCherry (0.5 μg) and the plasmid DNA (1.5 μg), containing the gene whose expression was to be detected, were mixed. Expression was analyzed 24 h post-transfection after fixing and immunostaining cells with the desired antibodies as described (18).

Immunoprecipitation Assay—For immunoprecipitation analysis, HEK293T cells were grown to 40% confluence in 10-cm dishes and transfected with 10 μg of Cx32-WT-EGFP, Cx32Δ220-EGFP, Cx32-WT-Myc, and Cx32Δ220-Myc either alone or in combination. Twenty-four hours post-transfection, the cells were harvested and lysed in a non-denaturing lysis buffer containing 1% Nonidet P-40, 1% TX-100, 1 mM $CaCl_2$, 1 mM PMSF, 2 mM Na_3VO_4, 1 mM NaF, and a protease inhibitor mixture. After lysis and protein estimation, 500 μg of total protein were mixed with 180 μl of IgG-Sepharose beads (MP Biomedicals, LLC, Santa Ana, CA) preincubated with anti-GFP antibody (Clontech) and incubated at 4 °C for 2 h. After incubation, the Sepharose-bound immune complexes were washed 5 times with the wash buffer (10 mM Tris-HCl, pH 7.5, 150 mM NaCl, and 0.5% Tween 20). The pulldown proteins were eluted with 2× Laemmli sample buffer and analyzed by SDS-PAGE and Western blotting with anti-Myc (Covance, Princeton, NJ) and anti-GFP antibodies.

Communication Assays—Gap junctional communication was assayed by microinjecting the fluorescent tracers Lucifer yellow (M_r 443, lithium salt); Alexa 488 (M_r 570, A-10436), or Alexa 594 (M_r 760, A-10438) (19, 21, 23, 24). Alexa dyes were purchased from Molecular Probes (Carlsbad, CA), and stock solutions (10 mM) for microinjection were prepared in water. Eppendorf InjectMan and FemtoJet microinjection systems (models 5271 and 5242, Brinkmann Instrument, Inc. Westbury, NY) mounted on a Leica DMIRE2 microscope were used to microinject the fluorescent tracers. Junctional transfer of the fluorescent tracers was assessed by counting the number of fluorescent cells (excluding the injected one) either at 1 min

Downloaded from http://www.jbc.org/ at University of NE Medical Center on December 30, 2015

(Lucifer yellow), 3 min (Alexa 488), or 15 min (Alexa 594) after microinjection into test cells as described (16, 18, 19, 25).

Live-cell Imaging and Fluorescent Recovery after Photobleaching—Bx32-WT-EGFP and Bx32Δ220-EGFP cells were seeded in LabTek FluoroDish culture dishes and allowed to grow to confluence. Confluent monolayers of cells were imaged using a 100× oil objective (NA 1.4) and a broad-band GFP filter. Cells were imaged at 37 °C in an atmosphere of 5% CO_2, 95% air in a live-cell imaging chamber mounted on an Olympus IX81 Spinning Disc Inverted Confocal motorized inverted microscope (Olympus America Inc.; Center Valley, PA). The microscope was controlled by IX2-UCB U-HSTR2 motorized system with a focus drift compensatory device IX1-ZDC. Images were captured using a Hamamatsu ORCA ER2 CCD camera and processed by imaging software Slidebook Version 5.0 (Intelligent Imaging Innovations, Denver, CO). z-stacks of 1 μm were acquired every 2 min for 120 min. The z-stacks (8) were projected into one single Z-projection that was superimposed on to a phase-contrast image.

For FRAP analysis, Bx32-WT-EGFP and Bx32Δ220-EGFP cells were photo-bleached as described (26). For measuring recovery within gap junction plaques, only puncta at the areas of cell-cell contact were photo-bleached, whereas recovery in non-junctional areas was determined in single cells in regions of the cells where only diffuse GFP fluorescence was observed, and there were no vesicular puncta. Recovery was measured using a Marianas Live Cell microscopy system (Intelligent Imaging Innovations Inc., Denver, CO) equipped with a Stanford Research Laser Ablation System (Model NL100). After the cells were photo-bleached, we captured z-stack images every 10 s for 15–20 min. As described in our earlier studies (26), before quantitation of relative fluorescence intensity raw images were de-convolved and collapsed into a projection image. For comparing multiple FRAP experiments, we collected normalized FRAP data using SlideBook (Version 5.0). For determining the relative fluorescence intensity value, we set the pre-bleach and post-bleach values as 100 and 0%, respectively. The graphs shown in Fig. 11 represent the plotted relative fluorescence intensity, and *error bars* represent the 95% confidence interval.

RESULTS

Cytoplasmic Tail-deleted Cx32 Assembles into Smaller Gap Junctions—Earlier studies had shown that the truncation of Cx32-CT up to amino acid 219 had no effect on the trafficking of connexons to the plasma membrane (27). We also showed that the cytoplasmic tail-deleted Cx32, abbreviated as Cx32Δ220, formed smaller gap junctions in human prostate cancer cell line LNCaP compared with full-length Cx32, hereafter abbreviated as Cx32-WT (18). Moreover, we further showed that in human squamous carcinoma cell line, A431D, Cx32-WT assembled into gap junctions only when cells acquired a partially polarized state, whereas Cx32Δ220 did not (19). These observations hinted that the Cx32-CT was involved in some aspect of gap junction plaque growth and/or initiation.

To define the role of Cx32-CT further, we retrovirally expressed Cx32-WT and Cx32Δ220 in LNCaP and BxPC3 cells in parallel and obtained pooled polyclonal cultures from each cell line. The pooled polyclonal cultures of LNCaP and BxPC3 cells expressing Cx32-WT and Cx32Δ220 are designated as LN32-WT, Bx32-WT, LN32Δ220, and Bx32Δ220 cells. Western blot analysis showed that Cx32-WT and Cx32Δ220 were expressed robustly in LNCaP and BxPC3 cells (Fig. 1, *A* and *B*). However, immunocytochemical analysis revealed that in both cell types Cx32Δ220 formed only small junctions, whereas Cx32-WT formed both large and small gap junctions (Fig. 1*C*; compare the size of gap junction puncta in *left panels* with the *right panels*). The small size of gap junctions formed by Cx32Δ220 was not related to the expression level as assessed by analyzing several individual clones of LNCaP and BxPC3 cells that differed in expression level by 2–4-fold (data not shown). We, therefore, measured the surface areas of 350–500 individual gap junctional puncta in LNCaP and BxPC3 cells expressing Cx32-WT and Cx32Δ220 (Fig. 1*D*). As described earlier, although the limit of resolution of light microscopy cannot distinguish multiple smaller junctions from a single larger gap junction, we counted each punctum at the cell-cell interface, as delineated by E-cadherin or β-catenin staining, as a single gap junction for quantification purposes (19, 28). We found that compared with LN32-WT and Bx32-WT cells, LN32Δ220 and Bx32Δ220 cells formed 20–35-fold smaller gap junctions (Fig. 1*D*). Moreover, the frequency of larger gap junctions was decreased in LN32Δ220 cells, with a concomitant increase in the frequency of smaller gap junctions. Furthermore, we found that the number of gap junctions per interface was more in cells expressing Cx32Δ220 compared with cells expressing Cx32-WT (data not shown). In addition, the number of intracellular puncta appeared to be more in cells expressing Cx32Δ220 compared with cells expressing Cx32-WT (Fig. 1*C*, *bottom right panel*). For example, the mean number of intracellular puncta in LN32-WT and Bx32-WT cells, respectively, was 7 ± 2 ($n = 35$) and 13 ± 4 ($n = 35$), whereas the mean number of intracellular puncta in LN32Δ220 and Bx32Δ220 cells was 25 ± 3 ($n = 15$) and 50 ± 10 ($n = 17$), respectively.

Function and the Detergent Solubility of Gap Junctions Composed of Cx32-WT and Cx32Δ220—To determine if Cx32Δ220 formed functional gap junctions, we microinjected gap junction-permeable fluorescent tracers into LN32-WT and LN32Δ220 cells. We found that the junctional transfer of all fluorescent tracers was reduced in cells expressing Cx32Δ220 (Fig. 2*A*; Table 1). To substantiate the immunocytochemical data, we determined gap junction assembly biochemically by measuring the solubility of Cx32-WT and Cx32Δ220 in TX100 (29). We found that a proportion of Cx32-WT and Cx32Δ220 was detected in detergent-insoluble and -soluble fractions in both LNCaP and BxPC3 cells (Fig. 2*B*). The detergent solubility of E-cadherin, an adherens junction-associated protein, was used as a control for these experiments. For example, we found that in three independent experiments between 40 and 50% of total Cx32-WT was in the TX100-insoluble fraction in LN32-WT and Bx32-WT cells, whereas this fraction ranged between 20 and 30% for LN32Δ220 and Bx32Δ220 cells. However, this difference in detergent-soluble and -insoluble fraction between Cx32-WT and Cx32Δ220 in LNCaP and BxPC3 cells was not statistically significant because of a large variation in soluble and insoluble fractions.

Downloaded from http://www.jbc.org/ at University of NE Medical Center on December 30, 2015

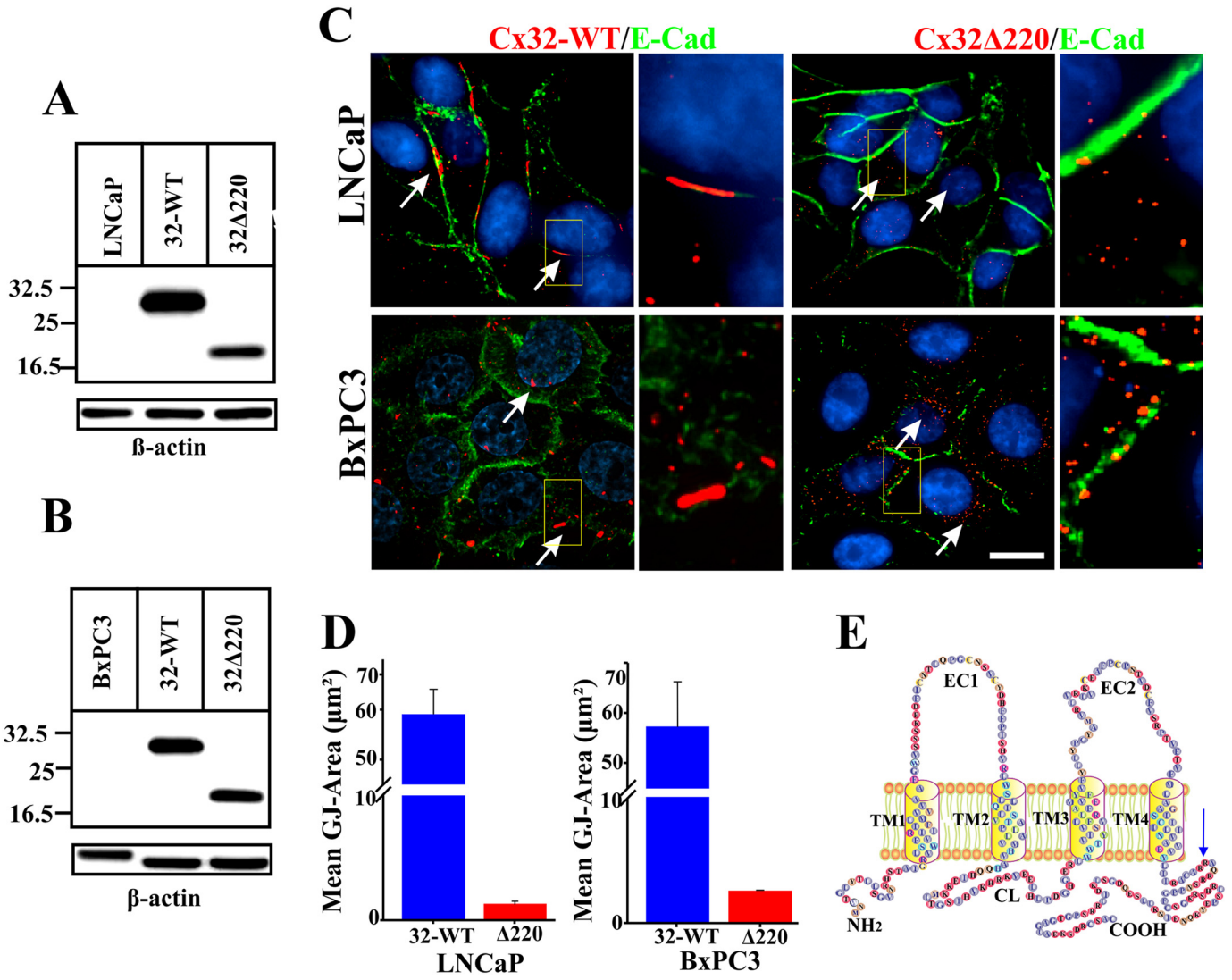

FIGURE 1. **Cytoplasmic tail-deleted Cx32 assembles into small gap junctions.** LNCaP and BxPC3 cells were infected with the control and Cx32-harboring recombinant retroviruses, and Cx32 expression level was determined by Western blot (*A* and *B*) and immunocytochemical analyses (*C* and *D*). *A*, note that only cells infected with Cx32-harboring retroviruses express Cx32-WT (*32-WT*) and Cx32Δ220 (*32Δ220*) in LNCaP (*A*) and BxPC3 (*B*) cells. The *numbers on the left* indicate the position of the molecular weight markers. An upward shift in the β-actin band in *B* is likely due to the presence of air bubbles at the interface of the gel and the running buffer. *C*, cells expressing Cx32-WT and Cx32Δ220 were immunostained for Cx32 with antibody raised against the cytoplasmic loop of Cx32. Note that, as indicated by *arrows*, Cx32-WT-expressing LNCaP (*upper row*, *left panels*) and BxPC3 (*lower row*, *left panels*) cells form large gap junctions (*red*), whereas Cx32Δ220-expressing LNCaP (*upper row*, *right panels*) and BxPC3 cells (*bottom row*, *right panels*) form miniscule gap junctions (*red*). The *enlarged images of the boxed areas in upper and lower panels* are shown toward the *left*. Immunostaining for E-cadherin (*E-Cad*, *green*) was used to delineate the cell-cell interfaces. The nuclei (*blue*) were stained with DAPI. *Bar* = 10 μm. *D*, gap junction areas of LNCaP and BxPC3 cells expressing Cx32-WT and Cx32Δ220. Areas (mean ± S.E.) of 350 distinct gap junction puncta from three single optical sections from three independent experiments after iterative volume de-convolution of the captured images were determined using the measurement module of Volocity. The area is represented in μm^2 (see "Materials and Methods"). Note the 20–35-fold decrease in the mean gap junction plaque area in cells expressing Cx32Δ220. The mean surface area of gap junctions composed of Cx32-WT was 58.5 ± 7.3 μm^2 and 56.4 ± 9.3 μm^2 for LNCaP-32 and Bx32-WT cells, respectively. The differences in areas between Cx32-WT and Cx32Δ220-expressing cells were statistically highly significant ($p \leq 0.001$). *GJ-Area*, gap junction area. *E*, topology of Cx32. The site at which Cx32 was truncated is indicated by the *arrow*. *TM1-TM4* = four transmembrane domains. *EC1* and *EC2*, extracellular loop 1 and 2; *CL*, cytoplasmic loop. NH_2 and COOH are the amino and the carboxyl termini.

To assess the relevance of our findings in LNCaP and BxPC3 cells to other cell types, we also retrovirally expressed Cx32-WT and Cx32Δ220 in HEK293T and HeLa cells as well as in another human pancreatic cancer cell line HPAF-II. We found that compared with Cx32-WT, Cx32Δ220 was assembled into smaller gap junction-like puncta in all cell types examined (data not shown). Thus, Cx32Δ220 assembled into smaller gap junction-like puncta in a variety of cell types. Overall, the above data suggest that although the size of gap junction plaques and function composed of cytoplasmic tail-deleted Cx32Δ220 are compromised, Cx32-CT is not required for initiating the formation of gap junctions.

Cx32-WT and Cx32Δ220 Traffic and Degrade Normally—To determine whether Cx32Δ220 trafficked normally to the cell surface, we used cell surface biotinylation. The data showed that Cx32Δ220 was biotinylated as efficiently as Cx32-WT in both cell types (Fig. 3*A*). For example, in both cell types between 5 and 10% of input Cx32-WT and Cx32Δ220 was biotinylated (see the Fig. 3*A* legend). To investigate if cell surface-associated Cx32Δ220 degrades more rapidly compared with Cx32-WT,

Downloaded from http://www.jbc.org/ at University of NE Medical Center on December 30, 2015

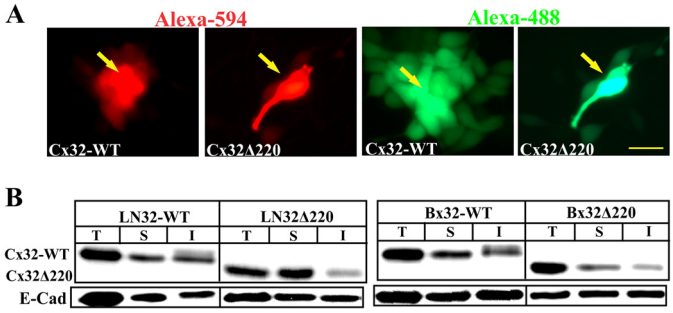

FIGURE 2. **Cx32-WT and Cx32Δ220 are assembled into detergent-insoluble functional gap junctions in LNCaP and BxPC3 cells.** *A*, LNCaP cells expressing Cx32-WT and Cx32Δ220 were microinjected with Alexa 488 (*green*, M_r 570) and Alexa 594 (*red*, M_r 760). Note extensive transfer of both tracers in LNCaP cells expressing Cx32-WT and weaker transfer in cells expressing Cx32Δ220. The microinjected cells are marked by the *arrows*. *Bar* = 20 μm. *B*, cells expressing Cx32-WT and Cx32Δ220 were grown in 10-cm dishes for 5–7 days. A TX100 solubility assay was used to measure the assembly of Cx32-WT and Cx32Δ220 into gap junctions. TX100 solubility of E-cadherin (*E-Cad*) was used as a control. Note that both Cx32-WT and Cx32Δ220 are found in TX100-soluble and TX100-insoluble fractions.

TABLE 1

Junctional transfer of fluorescent tracers in LN32-WT and LN32Δ220 cells

Cells, seeded in 6-cm dishes in replicate, were grown for 4–7 days to 70% confluence. Junctional transfer was measured after microinjecting fluorescent tracers (see "Materials and Methods").

Junctional tracer	Experiment number	Junctional transfer[a]	
		LN32	LN32Δ220
Lucifer yellow	1	26 ± 4 (18)	7 ± 2 (14)
	2	29 ± 6 (16)	6 ± 2 (13)
Alexa 488	1	22 ± 5 (16)	6 ± 2 (14)
	2	23 ± 6 (14)	8 ± 3 (18)
Alexa 594	1	13 ± 3 (14)	4 ± 1 (22)
	2	11 ± 4 (17)	3 ± 1 (29)

[a] The number of fluorescent cell neighbors (mean ± S.E.) at 1 min (Lucifer yellow), 3 min (Alexa 488), and 15 min (Alexa 594) after microinjection into test cells. The total number of injection trials is shown in parentheses.

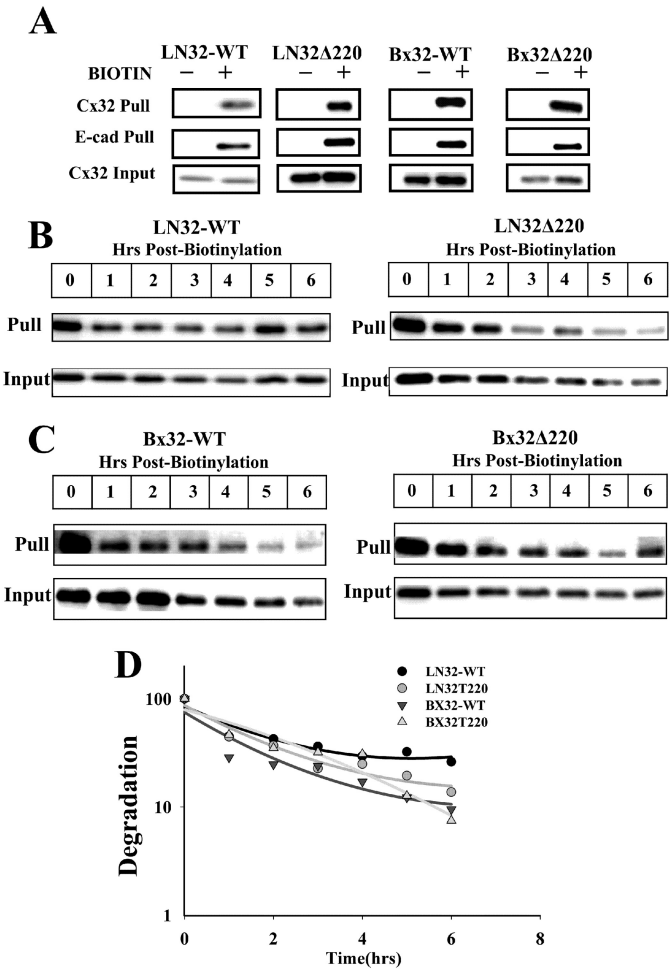

FIGURE 3. **Cx32-WT and Cx32Δ220 traffic and degrade normally in LNCaP and BxPC3 cells.** *A*, the cell surface proteins of LNCaP and BxPC3 were biotinylated and pulled (*Pull*) down by immobilized streptavidin and immunoblotted for Cx32. Biotinylation of E-cadherin (*E-cad*) was used as a positive control. A non-biotinylated dish was kept as a control (−). For input, 10 μg of total cell lysate was used. Note that both Cx32-WT and Cx32Δ220 and E-cad are efficiently biotinylated. *B*, cell surface associated Cx32-WT and Cx32Δ220 degrade with similar kinetics in LNCaP and BxPC3 cells. Cells were biotinylated at 4 °C and were incubated for various times at 37 °C before streptavidin pulldown and Western blotting ("Materials and Methods"). Representative blots for Cx32-WT and Cx32Δ220 from LNCaP (*B*) and BxPC3 (*C*) cells are shown. *D*, the blots were quantified using C-digit, and the values from two independent experiments were plotted graphically with Sigma plot. Note that cell surface-associated biotinylated Cx32-WT and Cx32Δ220 (Cx32T220) degrade with similar kinetics in both cell lines. The values in the two independent experiments varied by ≤10%.

we determined their kinetics of degradation after biotinylation. We found that the cell surface-biotinylated Cx32Δ220 degraded with kinetics similar to Cx32-WT (Fig. 3, *B* and *C*). The data from two independent experiments, which varied by <10%, are plotted in Fig. 3*D*. These findings suggest that the assembly of Cx32Δ220 into smaller gap junctions was not caused by its impaired trafficking to the cell surface or its rapid internalization and degradation before assembly but by some mechanism that interfered with the growth of the gap junction plaques after they had been assembled.

Expression of Cx32-WT Rescues the Small Junction Phenotype of Cx32Δ220—Because Cx32Δ220 trafficked normally to the cell surface and degraded with kinetics similar to Cx32-WT, we asked if small junction phenotype of Cx32Δ220 could be rescued by providing the Cx32-CT in *cis* (as a part of Cx32-WT). Earlier studies had shown that the defective gap junction assembly of Cx43 in human pancreatic cancer cell lines was restored upon expressing endocytosis-deficient mutants of Cx43 in cells expressing endogenous full-length Cx43 and that restoration was caused by the formation of heteromers between them (20). We rationalized that Cx32-WT, by forming heteromers with Cx32Δ220, might increase the frequency of large gap junctions by providing Cx32-CT in *cis*. To test this notion we transiently expressed Myc-tagged Cx32-WT in LN32Δ220 and Bx32Δ220 cells and, conversely, Myc-tagged Cx32Δ220 in LN32-WT and Bx32-WT cells. Formation of gap junctions was examined immunocytochemically. We found that the expression of Myc-tagged Cx32-WT increased the size of gap junction formed by Cx32Δ220 in both LN32Δ220 and Bx32Δ220 cells (Fig. 4, *A* and *D*). Expression of Myc-tagged Cx32Δ220 in LN32Δ220 and Bx32Δ220 cells had no effect (data not shown). As determined by measuring the areas of 350 gap junction puncta at cell-cell interfaces, we found that the mean surface area of rescued Cx32Δ220 gap junctions was 15–20-fold larger compared with the mean area of gap junctions formed by the Cx32Δ220 alone (Fig. 4*D*). For comparison, gap junctions formed of Cx32-WT and Cx32Δ220 alone are also shown (Fig. 4*C*).

Downloaded from http://www.jbc.org/ at University of NE Medical Center on December 30, 2015

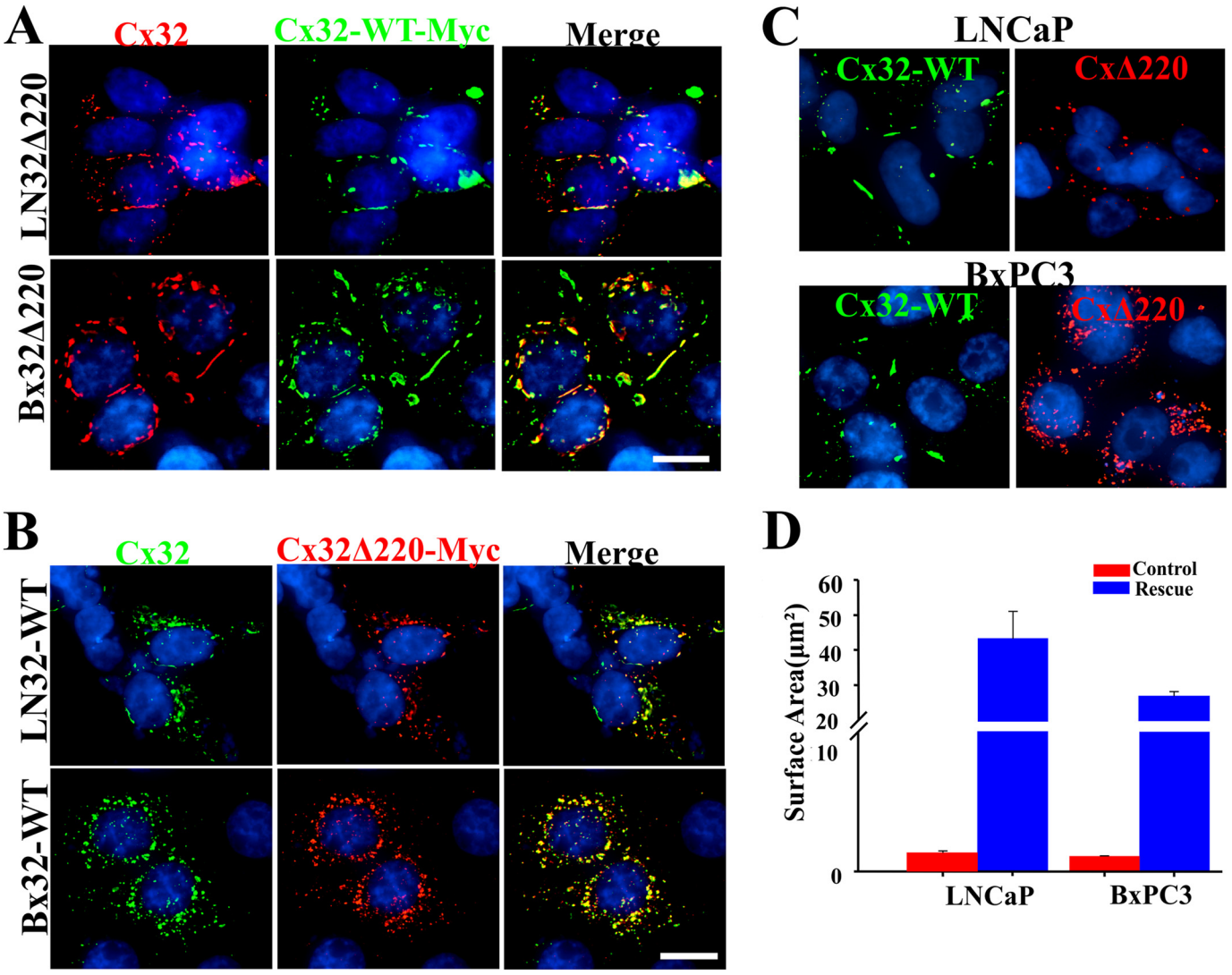

FIGURE 4. **Cytoplasmic tail of Cx32 controls gap junction size.** *A*, Myc-tagged Cx32-WT (*Cx32-WT-Myc*) was transiently expressed in LN32Δ220 (*top row*) and Bx32Δ220 (*bottom row*) cells, which express Cx32Δ220 stably. After 24 h, cells were immunostained for Myc (*green*) and Cx32 (*red*) using antibody raised against the cytoplasmic loop of Cx32 (amino acids 115–124). Note the formation of large gap junction plaques in cells expressing Cx32-WT-Myc compared with control cells that express only Cx32Δ220 (*C*, *right panels*). *B*, Myc-tagged Cx32Δ220 (*Cx32Δ220-Myc*) was transiently expressed in LN32-WT (*top row*) and Bx32-WT (*bottom row*) cells expressing Cx32-WT stably. After 24 h, cells were immunostained for Myc (*red*) and Cx32 (*green*) using antibody raised against the carboxyl tail of Cx32, which does not recognize Cx32Δ220. Note the loss of gap junction plaques in cells expressing Cx32Δ220 compared with control cells expressing Cx32-WT alone (*C*, *left panels*). *C*, gap junction size in cells expressing Cx32-WT (*Cx32-WT*, *green*) and Cx32Δ220 (*Cx32Δ220*, *red*) in LNCaP (*top row*) and BxPC3 (*bottom row*) cells transiently transfected with pmCherry and pAcGFP (not shown). *D*, mean surface area of the rescued gap junctions in LN32Δ220 and Bx32Δ220 cells in *A*. Areas (mean ±S.E.) of 350 distinct gap junction puncta from three single optical sections from three independent experiments after iterative volume de-convolution of the captured images were determined using the measurement module of Volocity. The area is represented in μm^2 (see "Materials and Methods"). Note the 15–20-fold increase in the mean gap junction plaque area in cells expressing Cx32-WT-Myc.

In the next series of experiments we examined if expression of Myc-tagged Cx32Δ220 in LN32-WT and Bx32-WT cells would attenuate the assembly of Cx32-WT into gap junctions. The results showed that the assembly of Cx32-WT was inhibited upon expressing Cx32Δ220-Myc (Fig. 4*B*). Expression of Myc-tagged Cx32-WT in LN32-WT and Bx32-WT had no effect (data not shown). As assessed visually, we also found that the rescue of Cx32Δ220 gap junctions was accompanied with a concomitant decrease in the number of intracellular puncta (Fig. 4*A*), whereas inhibition of Cx32-WT assembly was accompanied with a concomitant increase in intracellular puncta (Fig. 4*B*). To substantiate these observations, we counted the number of intracellular puncta from three independent microscopic fields in two independent experiments. We found that the mean number of intracellular puncta in LN32Δ220 and Bx32Δ220 cells was 27 ± 5 (n = 28) and 42 ± 8 (n = 35), respectively, which decreased to 17 ± 4 (n = 35) and 8 ± 4 (n = 27) in cells expressing Cx32-WT-Myc, respectively. Similarly, the mean number of intracellular puncta in LN32-WT and Bx32-WT cells was 6 ± 4 (n = 27) and 9 ± 4 (n = 27), respectively, which increased to 30 ± 4 (n = 15) and 42 ± 4 (n = 15), respectively, in cells expressing Cx32Δ220.

As assessed visually by light microscopy we also found that total Cx32 (WT and Δ220) co-localized nearly completely with the Myc-tagged reciprocal counterparts (Fig. 4*A*).). If Cx32-WT and Cx32Δ220 did not form heteromers with Cx32Δ220-Myc and Cx32-WT-Myc, it is less likely that the colocalization would have been as robust. These results suggest

Downloaded from http://www.jbc.org/ at University of NE Medical Center on December 30, 2015

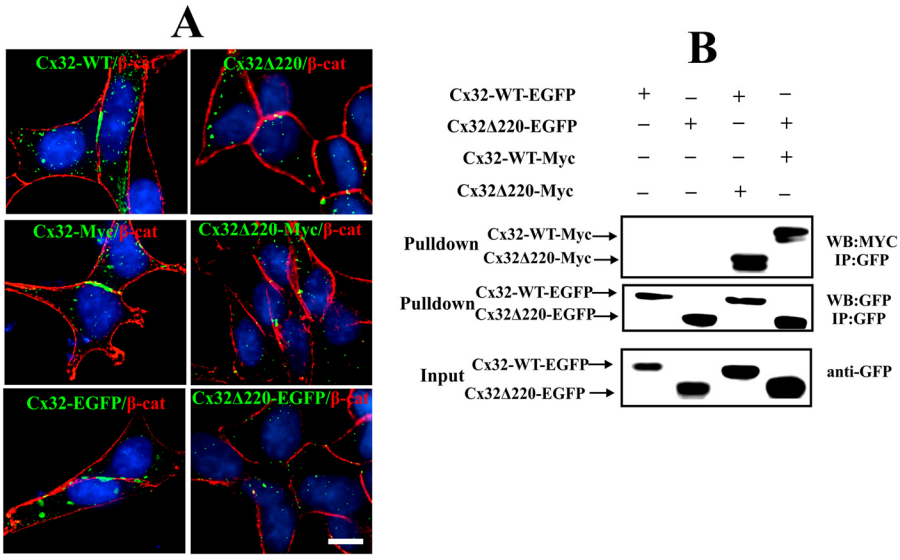

FIGURE 5. **Cx32-WT and Cx32Δ220-tagged with Myc or EGFP are assembled into gap junctions and co-immunoprecipitate each other.** *A*, Cx32-WT-Myc and Cx32Δ220-Myc, Cx32-WT-EGFP, and Cx32Δ220-EGFP were retrovirally expressed in LNCaP cells, and pooled polyclonal cultures were immunostained for Cx32, Myc, β-catenin (*β-cat*). *Top panels*: Cx32 (*green*) and β-catenin (*red*). *Middle panels*: Myc (*green*) and β-catenin (*red*). *Bottom panel*: β-catenin (*red*) alone. Note that tagged Cx32-WT and Cx32Δ220 are assembled into gap junctions like their untagged counterparts and the addition of tags had no effect on gap junction size. *Bar* = 10 μM. *B*, HEK293T cells were transfected with Cx32-WT-EGFP and Cx32Δ220-EGFP either alone or in combination with Cx32Δ220-Myc and Cx32-WT-Myc, respectively. EGFP-tagged proteins were pulled down with immobilized anti-GFP antibody and immunoblotted (*WB*) for anti-Myc and anti-GFP antibodies. Note that Cx32-WT-Myc co-immunoprecipitated (*IP*) with Cx32Δ220-GFP and Cx32Δ220-Myc with Cx32-WT-EGFP, indicating that both Cx32-WT and Cx32Δ220 form heteromers with each other. The *arrows* indicate the position of Cx32-WT and Cx32Δ220 on Western blots for pulldown and input lanes.

that the rescue likely occurs through the formation of heteromers, although light microscopy cannot distinguish between gap junctions composed of mixture of homomeric and heteromeric connexons. To test if adding EGFP or Myc tags to Cx32-WT and Cx32Δ220 affects their ability to assemble into gap junctions, we first retrovirally expressed Cx32-WT-EGFP, Cx32-WT-Myc, Cx32Δ220-EGFP, and Cx32Δ220-Myc in LNCaP cells. We found that neither tag had a discernible effect on the formation of gap junctions (Fig. 5*A*). Hence, to substantiate the immunocytochemical data, we transiently expressed both Cx32-WT-Myc and Cx32Δ220-Myc along with Cx32Δ220-EGFP and Cx32-WT-EGFP, respectively, in HEK293 cells. We then examined if the differentially tagged proteins could be co-immunoprecipitated from the detergent-soluble fraction, which likely contains only connexons that are not incorporated into gap junctional plaques (29). We used HEK293 cells for co-immunoprecipitation because of the low transfection efficiencies of BxPC3 and LNCaP. Moreover, HEK293 cells do not express Cx32 endogenously. The results showed that Cx32-WT and Cx32Δ220 reciprocally co-immunoprecipitated each other (Fig. 5*B*).

To test whether the preponderance of Cx32Δ220 or the ratio of Cx32-WT and Cx32Δ220 in a connexon controls gap junction assembly, we transiently expressed Cx32-WT and Cx32Δ220-EGFP at various ratios in HEK293T cells and examined assembly immunocytochemically (Fig. 6). For these experiments we used an antibody raised against the Cx32-CT that would not recognize Cx32Δ220-EGFP. As assessed by an increase in the size of gap junction formed by Cx32Δ220-EGFP and a concomitant decrease in the number of smaller gap junction puncta, we found that the rescue occurred only when the expression of Cx32-WT was high (Fig. 6*B*). Collectively, the data shown in Figs. 4, 5, and 6 suggest that Cx32-CT enhances the size of gap junctions.

Expression of Cx32-CT in Trans Affects Cx32Δ220 Junction Assembly—To explore whether expression of Cx32-CT by itself in *trans* would modulate the size of gap junctions formed by Cx32Δ220 or Cx32-WT, we rationalized that the Cx32-CT interacts and/or recruits proteins that determine the growth of plaques composed of Cx32Δ220 and that the recruitment and interaction occur at the cell surface. To test this, we engineered a Cx32-CT construct (representing amino acid residues 220–283) in which a myristoylation sequence was added at the amino terminus of Cx32-CT to target it to the plasma membrane; moreover, the Cx32-CT was also tagged with cyan fluorescent protein mTurquoise. This construct is designated as Cx32-CT-TQ-Myr (Fig. 7*A*). As a control, we also engineered an mCherry-Myr (*mCH-Myr*) construct in which the myristoylation sequence was added to the amino terminus of red fluorescent protein mCherry. Both engineered constructs were also tagged with Myc (Fig. 7*A*). Transient transfection of Cx32-CT-TQ-Myr and mCH-Myr in HEK293 cells followed by Western blot analysis showed that both Cx32-CT-TQ-Myr and mCH-Myr migrated at the predicted M_r and were appropriately targeted to the cell surface (data not shown).

To test if expression of Cx32-CT in *trans* would modulate gap junction size, we transiently expressed Cx32-CT-TQ-Myr and mCH-Myr in LN32-WT, LN32Δ220, Bx32-WT, and Bx32Δ220 cells and examined gap junction assembly immunocytochemically. As assessed by the size of the puncta at cell-cell interfaces, we found that although the expression of Cx32-CT-TQ-Myr had no effect on the assembly of Cx32-WT in LN32-WT and Bx32-WT cells, the small gap junction phenotypes of LN-32Δ220 and Bx32Δ220 cells were partially rescued

Downloaded from http://www.jbc.org/ at University of NE Medical Center on December 30, 2015

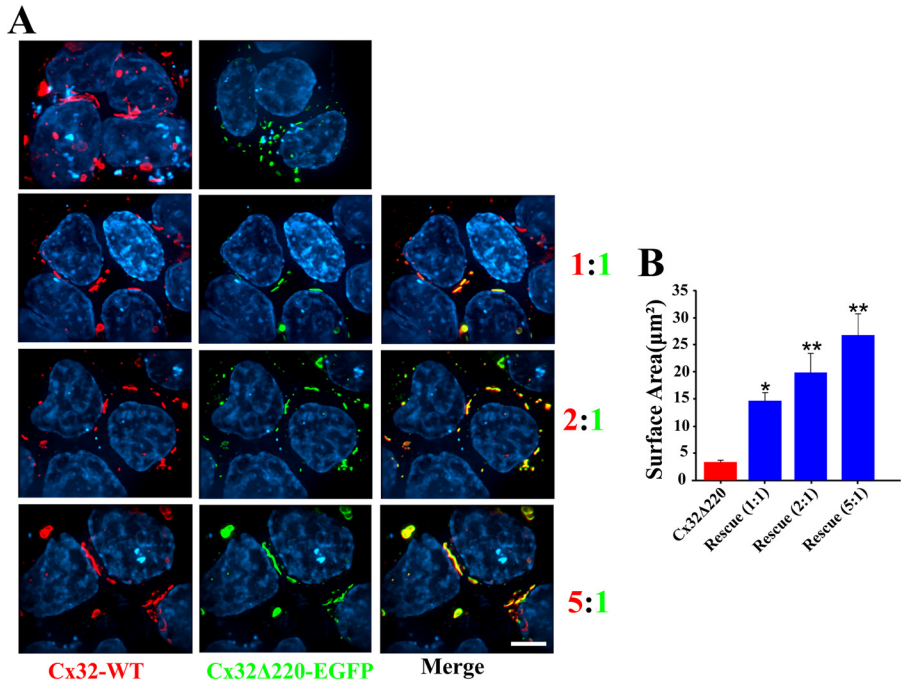

FIGURE 6. **An optimal expression of Cx32-WT and Cx32Δ220 is required to restore gap junction assembly.** *A*, HEK293T cells were transiently transfected with Cx32-WT and Cx32Δ220-EGFP at different ratios as indicated by the numbers on right. Transfected cells were fixed and immunostained for Cx32 (*red*) using antibody against the Cx32-CT. Note that cells expressing high levels of Cx32-WT are assembled into larger gap junctions. *B*, surface areas (mean ± S.E.) of gap junctions in cells transfected with Cx32-WT and Cx32Δ220-EGFP at the indicated ratios. The means represent areas from 100–150 individual puncta from 100–200-transfected cells. The *asterisk* (*) indicates a *p* value of ≤0.005, and *asterisks* (**) indicate a *p* value of ≤ 0.0001. A two tailed Student's *t* test was used to calculate *p* value assuming unequal variance.

(Fig. 7*B*). When we measured the surface areas of 350–670 individual gap junction puncta in transfected LN32Δ220 and BxΔ220 cells, there was a consistent 2–3-fold increase in the size (surface area) of gap junction puncta in LN32Δ220 and Bx32Δ220 cells expressing Cx32-CT-TQ-Myr compared with those expressing mCH-Myr (Fig. 7*C*). Moreover, we also found that the number of intracellular puncta in Cx32-CT-TQ-Myr expressing cells was significantly decreased (Table 2). These data suggest that Cx32-CT recruits some factor(s) to the cell surface as it traffics along the secretory pathway and/or upon arrival at the cell surface that facilitates the growth of gap junctions composed of Cx32Δ220.

Carboxyl Tail of Cx32 Is Essential for the Clustering of Cell-Cell Channels—Earlier studies had shown that clustering of cell-cell channels composed of Cx43 was induced when intracellular levels of cAMP were elevated (30–33). Moreover, other studies had shown that elevating intracellular cAMP level enhanced gap junctional communication by stabilizing Cx32 in rat hepatocytes (34, 35). These results, combined with our findings prompted us to investigate whether Cx32-CT is required for the clustering of cell-cell channels. Hence, we expected Cx32Δ220 not to cluster in response to forskolin, which elevates intracellular levels of cAMP by activating adenylyl cyclase (36). Therefore, we treated LN32-WT, LN32Δ220, Bx32-WT, and Bx32Δ220 with forskolin for 8 h based on our earlier studies with the other cell lines (37–39). The results (Fig. 8) showed the following. 1) Cell-cell channels composed of Cx32-WT clustered and/or redistributed to form large gap junctions in LN32-WT cells (Fig. 8, *left panels*). 2) The channels composed of Cx32Δ220 did not cluster at all in LN32Δ220 cells (Fig. 8, *right panels*). Similar results were obtained with Bx32-WT and Bx32Δ220 cells, although the effect was not robust because forskolin was toxic to these cells (data not shown). These results suggest that Cx32-CT is required for the clustering and/or redistribution of cell-cell channels and gap junction assembly.

Domains of the Carboxyl Tail of Cx32 That Determine Gap Junction Size—To determine which domain of Cx32-CT determines gap junction size, we engineered a series of Cx32 mutants with progressive truncation of the carboxyl tail (Fig. 9*A*). These mutants were then retrovirally expressed in LNCaP and BxPC3 cells. Western blot analysis showed that the mutants were expressed robustly and migrated at the predicted molecular weight (Fig. 9*B*). Immunocytochemical analysis revealed that the size of gap junctions formed by the mutants Cx32Δ270 and Cx32Δ250 was not discernibly different from those formed by Cx32-WT, whereas a robust decrease in gap junction size was seen with the mutants Cx32Δ230 and Cx32Δ220 (Fig. 9*C*). Taken together, these results suggest that the critical motifs that determine the size of gap junctions composed of Cx32 likely reside between residues 230 and 250 in the Cx32-CT.

Movement of Gap Junction Plaques Composed of Cx32-WT and Cx32Δ220—Next we investigated the dynamic behavior of gap junctions composed of Cx32-WT and Cx32Δ220 in LNCaP and BxPC3 cells. To test this we retrovirally expressed Cx32-WT-EGFP and Cx32Δ220-EGFP in LNCaP and BxPC3 cells. Like their untagged counterparts, Cx32-WT-EGFP and Cx32Δ220-EGFP were assembled into large and small gap junctions, respectively (Fig. 10, see also Fig. 5). Live-cell imaging was performed on confluent cells to allow unambiguous detection of gap junction plaques at the areas of cell-cell contact as well as

Downloaded from http://www.jbc.org/ at University of NE Medical Center on December 30, 2015

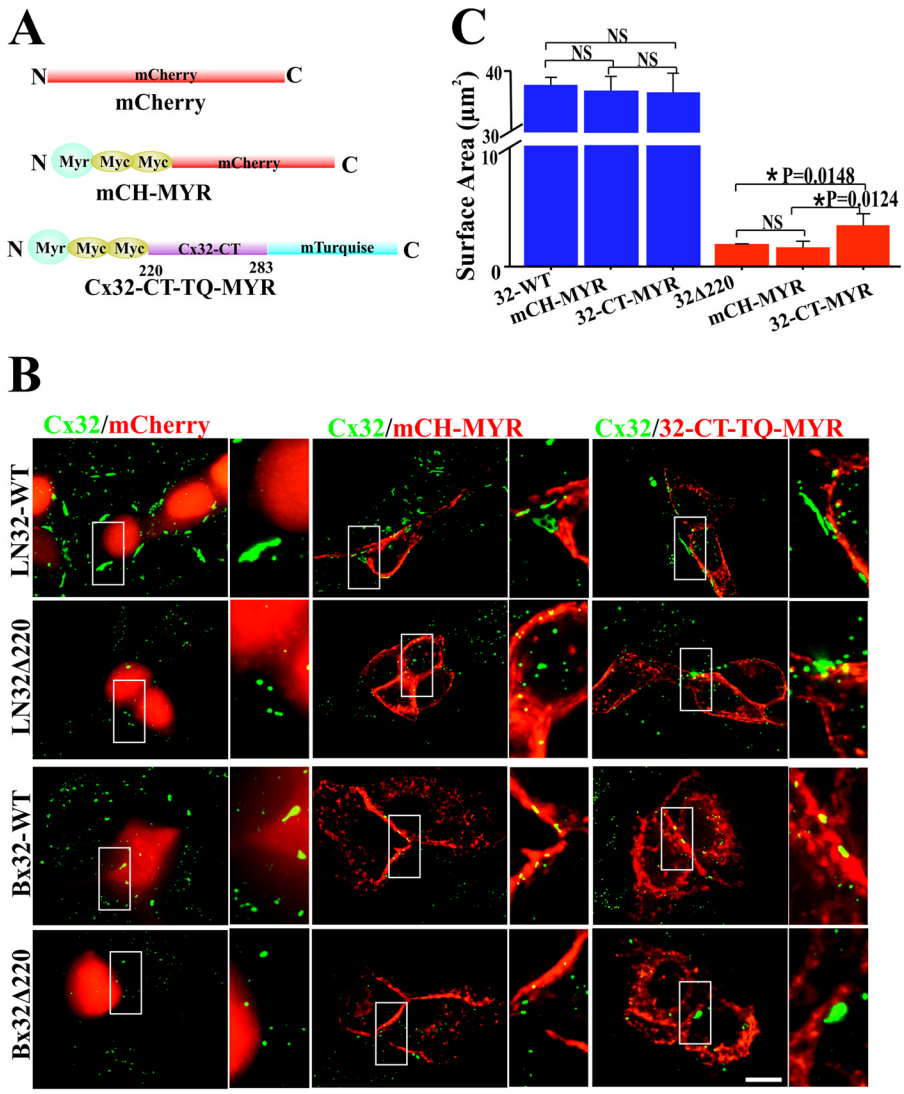

FIGURE 7. **Cx32-CT partially restores gap junction assembly.** *A*, a schematic diagram of the membrane-targeted mCherry and Cx32-CT constructs. Note that the membrane-targeted Cx32-CT construct contains monomeric Turquoise instead of mCherry (see "Materials and Methods"). *B*, LN32-WT, LN32Δ220, Bx32-WT, and Bx32Δ220 were transiently co-transfected with mCherry, mCherry-Myr (*mCH-MYR*), and Cx32-CT-Turquoise-Myr (*32-CT-TQ-MYR*). Cells were fixed and immunostained for Cx32 (*green*) 24 h after transfection. Note that only the expression of Cx32-CT-TQ-Myr increases the size of gap junction-like puncta. The color of the blue channels indicating the expression of Cx32-CT-TQ-MYR was converted to red to simplify the figure. *C*, areas (mean ±S.E.) of 350–670 distinct gap junction puncta from 3 single optical sections from 3 independent experiments in LNCaP cells after iterative volume de-convolution of the captured images were determined using the measurement module of Volocity. The area is represented in μm^2 (see "Materials and Methods"). Note the 2–3-fold increase in the mean gap junction plaque area in cells expressing Cx32-CT-TQ-MYR. The mean surface area of gap junctions composed of Cx32-WT was 37 ± 1.2 μm^2. The mean size of gap junctions composed of Cx32Δ220 was 1.5 ± 0.94 μm^2 for LN-32Δ220 cells transfected with mCH-MYR. *NS*, not significant.

TABLE 2

Expression of membrane-targeted Cx32-CT decreases number of intracellular puncta

LNCaP and BxPC3 cells stably expressing Cx32-WT (LN32-WT, Bx32-WT)) and Cx32Δ220 (LN32Δ220, Bx32Δ220) were transfected with membrane-targeted mCherry-Myr or Cx32-CT-TQ-Myr. The number of intracellular puncta was determined 24 h after transfection as described under "Materials and Methods." Numbers represent the mean ± S.E. Parenthesis indicate the number of transfected cells counted. Transfected cells were from 10 different fields in two independent experiments.

Transfection	LN32-WT	LN32Δ220	Bx32-WT	Bx32Δ220
mCherry-Myr	10.7 ± 4.1 (30)	18.7 ± 3.3 (25)	18.2 ± 3.8 (25)	18.6 ± 3.6 (42)
Cx32-CT-TQ-Myr	3.3 ± 1.0 (57)	8.1 ± 3.6 (62)	7.0 ± 4.3 (62)	6.2 ± 3.8 (57)

to minimize artifacts that might result from the movement of cells during imaging (see "Materials and Methods"). For most studies related to live-cell imaging, we utilized BxPC3 cells because they were easier to image compared with LNCaP cells. The results showed that gap junction plaques composed of Cx32Δ220-EGFP were highly dynamic compared with those composed of Cx32-WT-EGFP (supplemental Movies S1 and S2). By individually tracking the movement and disappearance of puncta at cell-cell contact areas, we found that most Cx32Δ220-EGFP puncta moved and disappeared within 10 min, whereas most Cx32-WT-EGFP gap junction puncta moved slowly and did not disappear even up to 2 h (Fig. 10, supplemental Movies S1 and S2). For example, the average speed of Cx32Δ220-EGFP puncta was twice that of Cx32-WT-

Downloaded from http://www.jbc.org/ at University of NE Medical Center on December 30, 2015

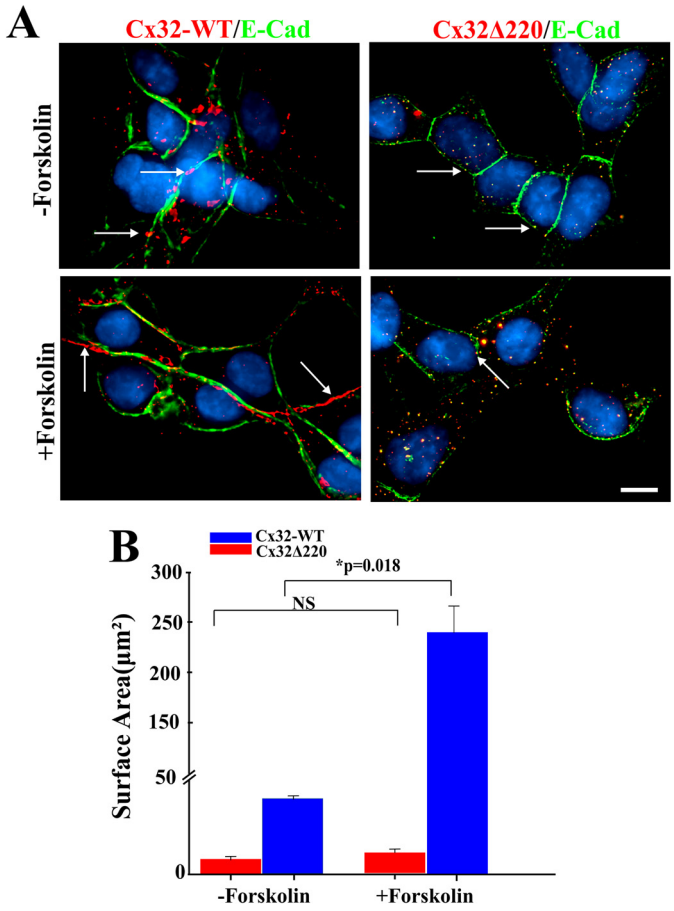

FIGURE 8. **Cx32Δ220 fails to cluster in response to forskolin.** *A*, LN32-WT and LN32Δ220 cells were treated with forskolin (+ *Forskolin*; 10 μM) for 8 h, and gap junction assembly was examined immunocytochemically. Controls (− *Forskolin*) were treated with 0.05% DMSO. Some gap junctions are indicated by the *white arrows*. Note that forskolin increased the size of gap junctions of Cx32-WT but not of Cx32Δ220 puncta. *Bar* = 10 μm. *B*, gap junction areas of Cx32-WT and Cx32Δ220-expressing LNCaP cells treated with forskolin as in *A*. Surface area (mean ± S.E.) of gap junctions composed of Cx32-WT (*blue*) and Cx32Δ220 (*red*) were determined with the measurement module of Volocity. Areas (mean ± S.E.) of 75–80 distinct gap junction puncta from 15 single optical sections from two independent experiments after iterative volume de-convolution of the captured images were determined using the measurement module of Volocity. The area is represented in μm^2 (see "Materials and Methods"). Note the 3–6-fold increase in the mean area of gap junctions composed of Cx32-WT (*blue*) in cells treated with forskolin. Note the lack of effect for gap junctions composed of Cx32Δ220 (*red*).

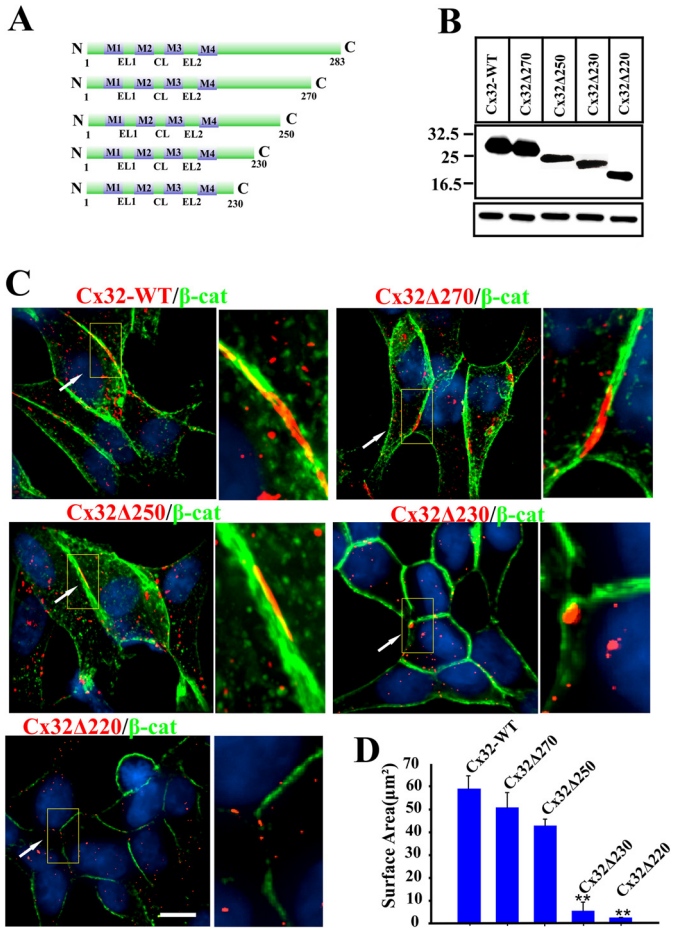

FIGURE 9. **Identification of the critical domain that determines gap junction size.** *A*, diagram showing Cx32 deletion mutants. The *numbers on the right* correspond to the number of the amino acid residue at which the truncation was introduced. *CL*, cytoplasmic loop; *EL1*, extracellular loop 1; *EL2*, extracellular loop 2. *B*, Western blot analysis of various mutants after transient transfection in HEK293T cells. The *numbers on the left* correspond to the position of the molecular weight markers. *C*, the mutants shown in *A* were retrovirally expressed in LNCaP cells, and pooled polyclonal cultures expressing the mutants stably were immunostained for Cx32 using antibody raised against the cytoplasmic loop of Cx32. Note that only cells expressing Cx32Δ220 and Cx32Δ230 form small gap junctions. *D*, surface area (mean ± S.E.) of 135–150 gap junctions composed of Cx32-WT, Cx32Δ270, Cx32Δ250, Cx32Δ230, and Cx32Δ220 were measured from three single optical sections from three independent experiments. The area is represented in μm^2. Note, there is a significant decrease in surface area of gap junctions composed of truncation mutants Cx32Δ230 and Cx32Δ220. The asterisks (**) indicate a *p* value of ≤0.0001. A two-tailed Student's *t* test was used to calculate *p* value assuming unequal variance. *Bar* = 10 μm.

EGFP puncta (Fig. 11*A*). We also measured the average speed of small puncta formed by the Cx32-WT-EGFP, comparable in size to those formed of Cx32Δ220-EGFP, and found that their speed was not significantly different from those formed by Cx32-WT-EGFP puncta (Fig. 11*A*). By analyzing the behavior of both large and small puncta of Cx32-WT-EGFP and several puncta of Cx32Δ220-EGFP, we found that Cx32Δ220-EGFP puncta moved abruptly, whereas the movement of large as well as small Cx32-WT-EGFP puncta was saltatory (supplemental Movies S1 and S2, Fig. 11*B*). Moreover, the puncta we imaged are less likely to be vesicles because their size was 2–3 times larger than the size of the vesicular puncta in the cytosol. Furthermore, most intracellular vesicular puncta lay at a different Z-plane and not only their spatiotemporal pattern of movement was different from those at cell-cell contact areas but also they could not be imaged together. Finally, it seems highly improbable that the EGFP-tagged cytoplasmic tail-deleted Cx32 aggregated nonspecifically, whereas the full-length Cx32 continued to assemble into gap junctions.

To assess if the mobility of Cx32Δ220-EGFP at the plasma membrane was different from Cx32-WT-EGFP, we photobleached gap junction plaques (contacting cells) and non-junctional areas (single cells) and measured recovery by FRAP analysis (Fig. 11, *C* and *D*, see "Materials and Methods"). The results showed that the mobile fraction of Cx32-WT-EGFP and Cx32Δ220-EGFP in gap junction plaques was low and was not different from each other (Fig. 11*C*). Moreover, the mobile fraction of both WT and cytoplasmic tail-deleted Cx32 in non-junctional areas was comparable with that observed in gap junction plaques (Fig. 11*D*). Earlier live-cell imaging studies had

Downloaded from http://www.jbc.org/ at University of NE Medical Center on December 30, 2015

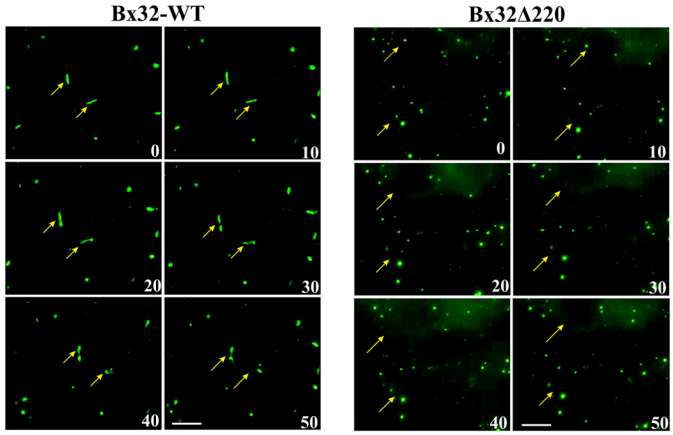

FIGURE 10. **Gap junctions composed of Cx32Δ220 are more mobile than those formed of Cx32-WT.** Selected time lapse images of BxPC3 cells expressing EGFP-tagged Cx32-WT (Bx32-WT) and Cx32Δ220 (Bx32Δ220) are shown. The tracked gap junction puncta are indicated by the *yellow arrows*. The *numbers in white* indicate lapsed time in minutes. Note the rapid disappearance of Cx32Δ220 puncta compared with Cx32-WT puncta. *Bar* = 10 μm.

indicated that the smaller gap junction-like puncta could fuse to give rise to larger puncta (40). Therefore, we also examined if larger plaques arose by fusion of the smaller plaques, a process that could be facilitated by the Cx32-CT. As assessed by analyzing the behavior of several large and small puncta composed of Cx32-WT-EGFP and Cx32Δ220-EGFP, we found that the small puncta rarely fused with one another (Table 3, supplemental Movies S1 and S2). Collectively, these data suggest that the Cx32-CT is not required for the mobility of Cx32 both in the plaques and in non-junctional regions.

DISCUSSION

The cytoplasmic tails of Cxs are highly divergent in amino acid composition, and phosphorylation of specific serines or tyrosines by a variety of kinases in the tails has been documented to be important in regulating the permeability of gap junctional channels (41). The cytoplasmic tails have also been shown to interact with many cytoskeletal and cell-junction-associated proteins (10). It is thought that, besides regulating the permeability of channels, these interactions govern the assembly of Cxs into gap junctions either directly or indirectly (10). Evidence favoring the role of cytoplasmic tails in controlling gap junction assembly has been obtained through colocalization and coimmunoprecipitation studies (10), and most studies have been performed with Cx43, which is ubiquitously expressed (2, 6). The extent to which the assembly of a particular Cx into gap junctions upon arrival at the cell surface is determined by factors intrinsic to the Cx itself or by extrinsic factors, such as the direct or indirect interaction of a Cx's cytoplasmic tail with the cytoskeleton or the cell surface-associated proteins, has not yet been explored mechanistically for many other Cxs (4, 10). The first major conclusion of our study is that the size of gap junction plaques composed of cytoplasmic tail-deleted Cx32Δ220 is drastically diminished and that the tail is not required for initiating the formation of a gap junction plaque but for its subsequent growth. The second major conclusion of our studies is that gap junctions composed of cytoplasmic tail-deleted Cx32 are highly unstable and that the tail of Cx32 is able to fine-tune the growth of a gap junction plaque when provided either in *cis* as a part of a connexon or in *trans* as a separate molecular entity targeted to the cell surface. Our findings suggest that the cytoplasmic tail is not required to initiate the assembly of Cx32 into gap junctions but for their subsequent growth and stability.

Our results showed that Cx32Δ220 not only trafficked normally to the cell surface but also degraded with kinetics similar to Cx32-WT (Fig. 3). Despite this, it formed 20–35-fold smaller gap junctions (Fig. 1, *C* and *D*). These data rule out impaired trafficking and/or enhanced degradation as one possible mechanism for the decrease in the size of gap junctions composed of Cx32Δ220. Moreover, gap junctions composed of Cx32Δ220 were also functional and detergent-resistant (Fig. 2, Table 1). These results suggest that the connexons formed of cytoplasmic tail-deleted Cx32Δ220 were able to dock and assemble into miniscule functional gap junctions and that the formation of nascent plaques is not dependent on the cytoplasmic tail, whereas the subsequent growth of the plaques is tail-dependent. Furthermore, although not directly demonstrated through electron microscopic studies, the puncta we have imaged at the site of cell-cell contact represent detergent-resistant functional gap junctions. Thus, these results strongly imply that the distinct puncta seen at the light microscopic level at the cell-cell contact sites likely represent gap junctional plaques rather than aggregates of undocked connexons (Fig. 1*C*). In this regard it is noteworthy to mention that the cytoplasmic tail-deleted Cx43 mutants, Cx43Δ244 and Cx43Δ258, were also assembled into gap junctions; however, the plaque growth composed of these mutants was not affected and compromised (42, 43). In fact, the average diameter of the plaques formed by the cytoplasmic tail-deleted Cx43Δ258 was larger than those formed by the full-length Cx43 (42). Given the fact that the expression of Cx32 is restricted to the polarized and differentiated cells of the exocrine glands (15), our results imply that the assembly of gap junctions composed of Cx32 is regulated differently from those composed of Cx43.

A salient as well as an intriguing aspect of our data is that the size of gap junctions composed of Cx32Δ220 was also increased 2–3-fold by expressing the membrane-targeted form of Cx32-CT (Cx32-CT-TQ-Myr) in *Trans* (Fig. 7). Moreover, increase in size of Cx32Δ220 puncta upon expressing Cx32-CT-TQ-Myr also decreased the number of intracellular puncta (Table 2). One possible explanation for these data is that Cx32-CT-TQ-Myr either sequesters a protein(s) at the cell surface that inhibits plaque growth and/or recruits additional proteins that facilitate growth. The latter possibility is supported by the Cx32-mediated recruitment of disc large protein, Dlg, to the cell surface in hepatocytes possibly through direct or indirect interaction (44, 45). Lack of a robust effect of Cx32-CT-TQ-Myr alone in incrementing Cx32Δ220 plaque growth compared with that observed upon expressing Cx32-WT may be due the time required by Cx32-CT-Myr, which is delivered randomly to the cell surface, to arrive near the connexons or plaques as compared with when Cx32-CT is available as a part of the connexon itself.

Earlier live-cell imaging studies had indicated that the smaller gap junction-like puncta could fuse to give rise to larger

Downloaded from http://www.jbc.org/ at University of NE Medical Center on December 30, 2015

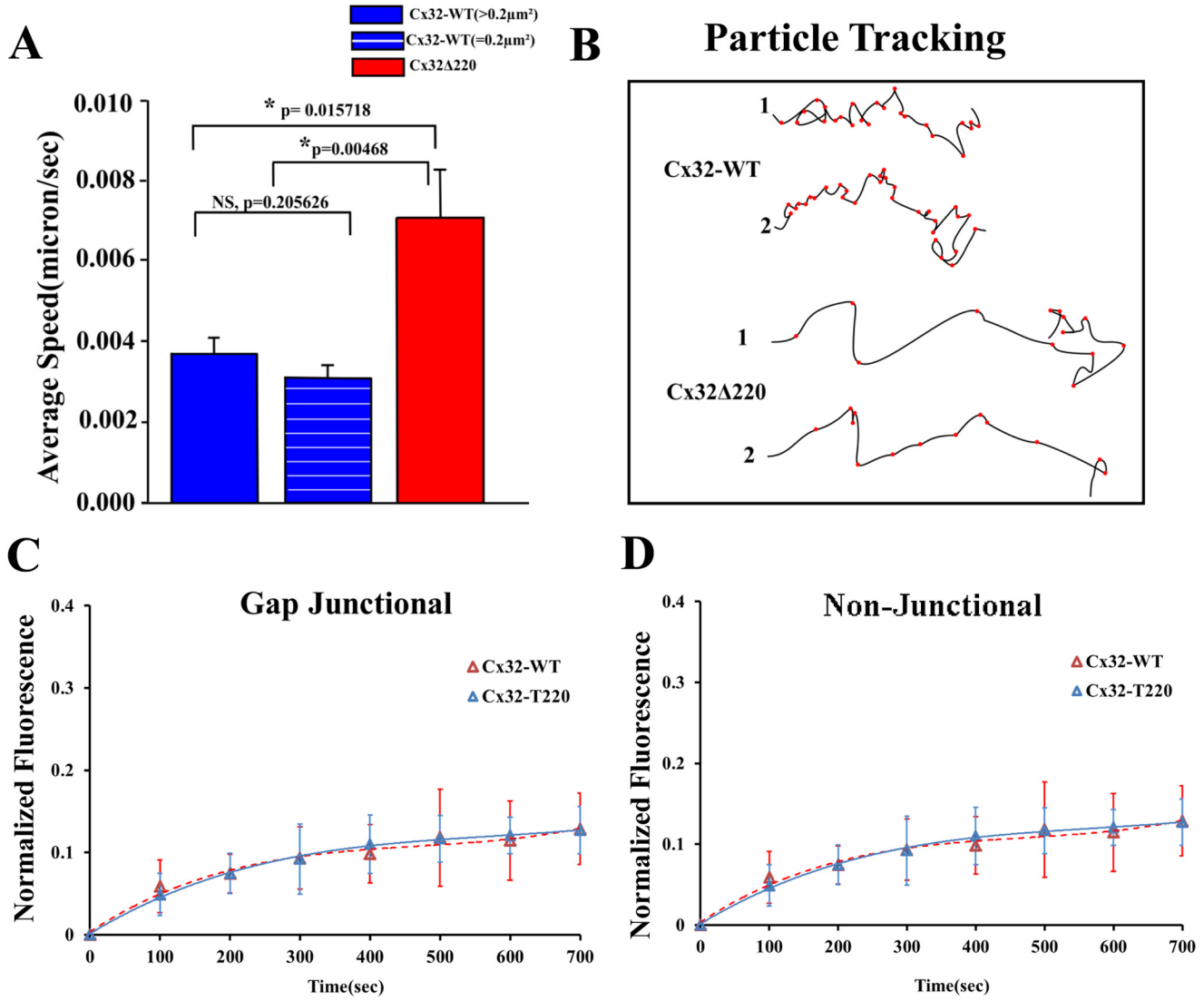

FIGURE 11. **Mobility of gap junctions and connexons composed of Cx32-WT and Cx32Δ220.** *A*, average (mean ± S.E.) speed of gap junction puncta composed of EGFP-tagged Cx32-WT and Cx32Δ220 in BxPC3 cells (n = 10). *NS*, not significant. *B*, motile behavior of gap junction puncta composed of EGFP-tagged Cx32-WT and Cx32Δ220 in BxPC3 cells as determined by tracking individual puncta (n = 5; only two are shown). Note that the average speed of gap junction puncta composed Cx32Δ220 is nearly twice that of puncta composed of Cx32-WT. Note also that Cx32-WT puncta comparable in size to Cx32Δ220 puncta also move slower. *C* and *D*, analysis of mobility fraction of Cx32-WT and Cx32Δ220 (Cx32-T220) by FRAP within gap junctional plaques in contacting cells (*C*, *Gap Junctional*) and in single cells (*D*, *Non-junctional*). Note that there is no difference in the mobile fraction of Cx32-WT and Cx32Δ220 in gap junction plaques and at non-junctional regions. In *C*, *Cx32-T220* = Cx32Δ220.

TABLE 3

Larger gap junctions do not arise from the fusion of microscopically detectable small gap junctions

Live cell imaging of BxPC3 and LNCaP cells expressing EGFP-tagged Cx32-WT and Cx32Δ220 was performed, and puncta that appeared at the cell-cell contact were individually tracked as described under "Materials and Methods." For Bx32-WT-EGFP and Bx32Δ220-EGFP the data were obtained from 5–8 independent live-cell imaging experiments. Numbers in parenthesis represent the % of total.

BxPC3 cells expressing	No. of puncta tracked	No. of puncta never fused	No. of puncta fused but separated	No. of puncta fused
		%		
Bx32-WT-EGFP	205	188 (92)	8 (4)	17 (8)
Bx32Δ220-EGFP	193	186 (96)	5 (2.6)	7 (3.6)
LN32Δ220-EGFP	105	101 (96)	6 (5.7)	8 (7.6)

puncta (40). Therefore, we also rationalized that the larger plaques arose from the fusion of the smaller plaques, a process that could be facilitated by the Cx32-CT. However, our live-cell imaging data revealed that this mechanism was less likely, as small puncta were rarely seen to fuse with one another (supplemental Movies S1 and S2, Table 3). Moreover, although our live-cell imaging data showed substantially decreased mobility of larger plaques formed of Cx32-WT-EGFP, we also found that gap junction-like puncta composed of Cx32Δ220-EGFP were highly mobile and moved faster and abruptly (Fig. 11*B*). Furthermore, even small gap junction-like puncta formed by the Cx32-WT-EGFP, comparable in size to those formed by

Downloaded from http://www.jbc.org/ at University of NE Medical Center on December 30, 2015

Cx32Δ220-EGFP, were as stable and sessile as larger puncta (Fig. 11*A*, supplemental Movies S1 and S2). In addition, our FRAP analysis showed that the mobility of both Cx32Δ220-EGFP and Cx32-WT-EGFP within gap junctional plaques (in contacting cells) and in non-junctional membranes (in single cells) was not discernibly different (Fig. 11, *C* and *D*). These results rule out differential diffusion of Cx32-WT and Cx32Δ220 connexons at the cell surface as one mechanism to account for the drastic difference in the size of gap junction plaques. In this regard it is noteworthy to mention that the mobility of gap junction-like puncta composed of cytoplasmic tail-deleted Cx43 was not different from Cx43-WT (43).

The findings that the small size of gap junctional plaques composed of Cx32Δ220 could be rescued upon co-expressing Cx32-WT and vice versa (Figs. 4 and 6) combined with the fact that the tail had no effect on the mobility of Cx32 raise intriguing possibilities with regard to the molecular mechanisms involved in the genesis of larger plaques and the role played by the Cx32-CT in plaque growth. Evidence to date supports the notion that once a plaque has been nucleated, the subsequent growth of a plaque occurs upon recruitment of connexons to its periphery either by diffusion (43, 46–48) or upon direct delivery of connexons to its vicinity (49). Moreover, it is highly likely that the docking of connexons to form functional cell-cell channels occurs either in the vicinity of the plaque with a concomitant incorporation of the channels into the plaque or concurrently (12, 50). What might then be the possible explanation for the failure of Cx32Δ220 to assemble into larger gap junctions?

The molecular collisions among several transmembrane proteins have been postulated to be regulated by the partitioning of the entire plasma membrane by the actin-based membrane cytoskeleton and its associated proteins into several subdomains (51). Anchoring of transmembrane proteins to the cytoskeleton proteins either directly or indirectly via a scaffolding protein is likely to hinder or prevent their diffusion in the plane of the plasma membrane compared with proteins that are not anchored (52–54). Thus, tethering of a Cx's cytoplasmic tail to the cytoskeleton directly or indirectly could attenuate the delivery of connexons to the plaque by hindering mobility on the plane of the membrane. Alternatively, tethering could stimulate plaque growth by anchoring connexons near the plaque to increase the probability of docking of connexons to form cell-cell channels with concomitant incorporation of the channels into the plaque. A similar mechanism may be evoked to explain the increased motility of small gap junctions composed of Cx32Δ220 and increased stability of plaques composed of Cx32-WT. In addition, the cytoplasmic tail might recruit some factors to the sites of nascent plaques to stabilize membrane subdomains near its vicinity to permit docking of connexons and the subsequent incorporation of channels in the plaque.

Several lines of evidence provide support for this notion. For example, earlier studies showed that when the interaction between the cytoplasmic tail of Cx43 and ZO-1, a scaffolding protein that links Cx43's cytoplasmic tail to the cytoskeleton, was disrupted, connexon recruitment and/or incorporation to the plaque periphery was facilitated, leading to an increase in the size of gap junction plaque (12). On the other hand, deletion of the PDZ-binding domain of Cx50, a Cx expressed in the lens epithelial cells and shown to interact with ZO-1 (55), inhibited gap junction assembly (13). Hence, it is possible that the cytoplasmic tail is required for anchoring Cx32 to cytoskeletal proteins near the plaque to facilitate docking of connexons between the contiguous cells and the subsequent incorporation of the channels into nascent plaque. Support for this line of thought comes from our data showing an increase in the size of gap junctions composed of Cx32Δ220 upon transient expression of Cx32-WT (Fig. 4*A*), a decrease in the size of gap junctions composed of Cx32-WT upon transient expression of Cx32Δ220 (Fig. 4*B*), and failure of Cx32Δ220, but not Cx32-WT, to cluster to form larger gap junctions upon elevation of intracellular levels of cAMP (Fig. 8). In this regard it is noteworthy to mention that in contrast to ubiquitously expressed Cx43, only a few proteins have been shown to interact with the cytoplasmic tail of Cx32. These proteins included SAP97/Dlg (44, 45), calmodulin (56, 57), ZO-1 (58), caveolin-1 (59), and occludin (60). However, in LNCaP and BxPC3 cells, none of these proteins except caveolin-1 co-localized with Cx32 as assessed by immunocytochemical analysis,[3] and hence their involvement in regulating the assembly of Cx32 into gap junctions is less likely. Our future studies will explore the role of caveolin-1 in regulating the assembly of Cx32 into gap junctions.

Based on the above arguments, we propose that the cytoplasmic tail of Cx32 is essential for the stability and subsequent growth of the plaque but is not required to initiate the formation of a gap junction plaque. Once the plaque has been nucleated, the tail permits the linkage of Cx32 to the cytoskeleton by mass action, which stabilizes the plaque. This permits more channels to be recruited and incorporated in the plaque. The nascent plaques formed by the cytoplasmic tail-deleted Cx32Δ220 remain unstable because they fail to establish a linkage with the cytoskeleton. The Cx32Δ220 plaques remain small because they are dislodged before a significant increment of connexons or channels occurs at the plaque periphery. This explanation is in accord with the increased stability of both the small and the large plaques formed of Cx32-WT. We also propose that the mobility of Cx32-WT in non-junctional areas away from the plaque is not dependent on the anchoring of the tail to the cytoskeleton. Earlier studies showed that in pig thyrocytes, which expressed endogenous Cx43 and Cx32 as well as in Cx43-expressing human embryonic kidney cells in which Cx26 was transiently expressed, although both Cxs were assembled into gap junctions, the plaques composed of each Cx subtype resided in two different plasma membrane subdomains (61, 62). Our results with Cx32Δ220 may provide a rational explanation for the segregation of plaques composed of Cx43 and Cx32 in different subdomains of the plasma membrane as well as for the increased motility of Cx26-GFP, a tail-less Cx, in gap junction-like clusters (47). Altogether, our results suggest that the assembly of Cx32 is regulated differently than that of Cx43 and substantiate the conclusion drawn from earlier studies which showed that the assembly of Cx32 and Cx43 into gap junctions was differentially regulated in cadherin-null human squamous carcinoma cells (19).

[3] P. Katoch, S. Mitra, A. Ray, L. Kelsey, B. J. Roberts, J. K. Wahl III, K. R. Johnson, and P. P. Mehta, unpublished observations.

Downloaded from http://www.jbc.org/ at University of NE Medical Center on December 30, 2015

What might be the possible physiological relevance of cytoplasmic-tail-mediated facilitation of gap junction assembly with regard to the growth of a plaque? The number of cell-cell channels in a given gap junction plaque varies substantially and may range from 50 to more than 10,000; moreover, there is a wide range of variation in the size of gap junctions formed between the two contiguous cells (5, 63). Furthermore, hormone-induced clustering of cell-cell channels to increase the size of gap junctions is frequently observed (15, 64). Clustering of cell-cell channels is a prerequisite for the opening of cell-cell channels and that the larger gap junctional plaques have more open channels compared with the smaller plaques (50). It is tempting to speculate that although post-translational modifications in the cytoplasmic tail of a Cx are used to acutely regulate gating of cell-cell channels, the engagement and the disengagement of a Cx tail with the cytoskeletal proteins are used for the chronic regulation of permeability of channels with slower, spatiotemporal characteristics. Alternatively, the cytoplasmic tail-mediated increase in gap junction plaque size and stability may facilitate the assembly of other junctional complexes that are required to maintain the polarized and differentiated state of epithelial cells (65, 66). More elaborate studies are needed to further assess the physiological significance of our findings with respect to functional role of gap junctional communication.

Acknowledgments—We thank Dr. Souvik Chakraborty for helpful discussion and suggestions. We thank Tom Dao for help with the live-cell imaging and Robert Svoboda for constructed membrane-targeted form of the cytoplasmic tail of connexin32. We also thank Drs. Steve Caplan and Naava Naslavsky for helpful suggestions regarding endocytosis throughout the course of this study. The live cell imaging studies were supported by the National Institutes of Health Phase III CoBRE Grant 5P30GM106397 (to K. R. J.).

REFERENCES

1. Goodenough, D. A., and Paul, D. L. (2009) Gap junctions. *Cold Spring Harbor Perspect. Biol.* **1,** a002576
2. Beyer, E. C., and Berthoud, V. M. (2009) in *Connexins: A Guide* (Harris, A., and Locke, D., eds.), pp. 3–26, Springer-Verlag New York Inc., New York
3. Dobrowolski, R., and Willecke, K. (2009) Connexin-caused genetic diseases and corresponding mouse models. *Antioxid. Redox Signal.* **11,** 283–295
4. Laird, D. W. (2010) The gap junction proteome and its relationship to disease. *Trends Cell Biol.* **20,** 92–101
5. Sosinsky, G. E., and Nicholson, B. J. (2005) Structural organization of gap junction channels. *Biochim. Biophys. Acta* **1711,** 99–125
6. Laird, D. W. (2006) Life cycle of connexins in health and disease. *Biochem. J.* **394,** 527–543
7. Foote, C. I., Zhou, L., Zhu, X., and Nicholson, B. J. (1998) The pattern of disulfide linkages in the extracellular loop regions of connexin 32 suggests a model for the docking interface of gap junctions. *J. Cell Biol.* **140,** 1187–1197
8. Zhou, L., Kasperek, E. M., and Nicholson, B. J. (1999) Dissection of the molecular basis of pp60(v-src) induced gating of connexin 43 gap junction channels. *J. Cell Biol.* **144,** 1033–1045
9. Harris, A. (2007) Connexin channel permeability to cytoplasmic molecules. *Prog. Biophys. Mol. Biol.* **94,** 120–143
10. Hervé, J. C., Derangeon, M., Sarrouilhe, D., Giepmans, B. N., and Bourmeyster, N. (2012) Gap junctional channels are parts of multiprotein complexes. *Biochim. Biophys. Acta* **1818,** 1844–1865
11. Hunter, A. W., Barker, R. J., Zhu, C., and Gourdie, R. G. (2005) Zonula occludens-1 alters connexin43 gap junction size and organization by influencing channel accretion. *Mol. Biol. Cell* **16,** 5686–5698
12. Rhett, J. M., Jourdan, J., and Gourdie, R. G. (2011) Connexin 43 connexon to gap junction transition is regulated by zonula occludens-1. *Mol. Biol. Cell* **22,** 1516–1528
13. Chai, Z., Goodenough, D. A., and Paul, D. L. (2011) Cx50 requires an intact PDZ-binding motif and ZO-1 for the formation of functional intercellular channels. *Mol. Biol. Cell* **22,** 4503–4512
14. Wei, C. J., Xu, X., and Lo, C. W. (2004) Connexins and cell signaling in development and disease. *Annu. Rev. Cell Dev. Biol.* **20,** 811–838
15. Bosco, D., Haefliger, J. A., and Meda, P. (2011) Connexins: key mediators of endocrine function. *Physiol. Rev.* **91,** 1393–1445
16. Mehta, P. P., Perez-Stable, C., Nadji, M., Mian, M., Asotra, K., and Roos, B. (1999) Suppression of human prostate cancer cell growth by forced expression of connexin genes. *Dev. Genet.* **24,** 91–110
17. Shen, M. M., and Abate-Shen, C. (2010) Molecular genetics of prostate cancer: new prospects for old challenges. *Genes Dev.* **24,** 1967–2000
18. Mitra, S., Annamalai, L., Chakraborty, S., Johnson, K., Song, X. H., Batra, S. K., and Mehta, P. P. (2006) Androgen-regulated formation and degradation of gap junctions in androgen-responsive human prostate cancer cells. *Mol. Biol. Cell* **17,** 5400–5416
19. Chakraborty, S., Mitra, S., Falk, M. M., Caplan, S. H., Wheelock, M. J., Johnson, K. R., and Mehta, P. P. (2010) E-cadherin differentially regulates the assembly of connexin43 and connexin32 into gap junctions in human squamous carcinoma cells. *J. Biol. Chem.* **285,** 10761–10776
20. Johnson, K. E., Mitra, S., Katoch, P., Kelsey, L. S., Johnson, K. R., and Mehta, P. P. (2013) Phosphorylation on Ser-279 and Ser-282 of connexin43 regulates endocytosis and gap junction assembly in pancreatic cancer cells. *Mol. Biol. Cell* **24,** 715–733
21. Govindarajan, R., Chakraborty, S., Johnson K. E., Falk, M. M., Wheelock, M. J., Johnson, K. R., and Mehta, P. P. (2010) Assembly of connexin43 is differentially regulated by E-cadherin and N-cadherin in rat liver epithelial cells. *Mol. Biol. Cell* **21,** 4089–4107
22. Mehta, P. P., Hotz-Wagenblatt, A., Rose, B., Shalloway, D., and Loewenstein, W. R. (1991) Incorporation of the gene for a cell-to-cell channel proteins into transformed cells leads to normalization of growth. *J. Membr. Biol.* **124,** 207–225
23. Govindarajan, R., Zhao, S., Song, X.-H., Guo, R.-J., Wheelock, M., Johnson, K. R., and Mehta, P. P. (2002) Impaired trafficking of connexins in androgen-independent human prostate cancer cell lines and its mitigation by a-catenin. *J. Biol. Chem.* **277,** 50087–50097
24. Kelsey, L., Katoch, P., Johnson, K. E., Batra, S. K., and Mehta, P. (2012) Retinoids regulate the formation and degradation of gap junctions in androgen-responsive human prostate cancer cells. *PLoS ONE* **7,** e32846
25. Mehta, P. P., Bertram, J. S., and Loewenstein, W. R. (1986) Growth inhibition of transformed cells correlates with their junctional communication with normal cells. *Cell* **44,** 187–196
26. Roberts, B. J., Reddy, R., and Wahl, J. K., 3rd (2013) Stratifin (14-3-3 s) Limits plakophilin-3 exchange with the desmosomal plaque. *PLoS ONE* **8,** e77012
27. Martin, P. E., Steggles, J., Wilson, C., Ahmad, S., and Evans, W. H. (2000) Targeting motifs and functional parameters governing the assembly of connexins into gap junctions. *Biochem. J.* **349,** 281–287
28. Gourdie, R. G., Green, C. R., and Severs, N. J. (1991) Gap junction distribution in adult mammalian myocardium revealed by an anti-peptide antibody and laser scanning confocal microscopy. *J. Cell Sci.* **99,** 41–55
29. VanSlyke, J. K., and Musil, L. S. (2000) Analysis of connexin intracellular transport and assembly. *Methods* **20,** 156–164
30. Atkinson, M. M., Lampe, P. D., Lin, H. H., Kollander, R., Li, X.-R., and Kiang, D. T. (1995) Cyclic AMP modifies the cellular distribution of connexin43 and induces a persistent increase in the junctional permeability of mouse mammary tumor cells. *J. Cell Sci.* **108,** 3079–3090
31. Paulson, A. F., Lampe, P. D., Meyer, R. A., TenBroek, E., Atkinson, M. M., Walseth, T. F., and Johnson, R. G. (2000) Cyclic AMP and LDL trigger a rapid enhancement in gap junction assembly through a stimulation of connexin trafficking. *J. Cell Sci.* **113,** 3037–3049
32. Mehta, P. P., Yamamoto M, and Rose B (1992) Transcription of the gene for the gap junctional protein connexin43 and expression of functional cell-to-cell channels are regulated by cAMP. *Mol. Biol. Cell* **3,** 839–850

Downloaded from http://www.jbc.org/ at University of NE Medical Center on December 30, 2015

33. Mehta, P. P., Lokeshwar, B. L., Schiller, P. C., Bendix, M. V., Ostenson, R. C., Howard, G. A., and Roos, B. A. (1996) Gap-junctional communication in normal and neoplastic prostate epithelial cells and its regulation by cAMP. *Mol. Carcinog.* **15,** 18–32
34. Sáez, J. C., Gregory, W. A., Watanabe, T., Dermietzel, R., Hertzberg, E. L., Reid, L., Bennett, M. V., and Spray, D. C. (1989) cAMP delays disappearance of gap junctions between pairs of rat hepatocytes in primary culture. *Am. J. Physiol.* **257,** C1–C11
35. Sáez, J. C., Nairn, A. C., Czernik, A. J., Spray, D. C., Hertzberg, E. L., Greengard, P., and Bennett, M. V. (1990) Phosphorylation of connexin 32, a hepatocyte gap-junction protein, by cAMP-dependent protein kinase, protein kinase C and Ca^{2+}/calmodulin-dependent protein kinase II. *Eur. J. Biochem.* **192,** 263–273
36. Seamon, K. B., and Daly, J. W. (1981) Forskolin: a unique diterpene activator of cyclic AMP-generating systems. *J. Cyclic Nucleotide Res.* **7,** 201–224
37. Wang, Y., and Mehta, P. P. (1995) Facilitation of gap junctional communication and gap junction formation by inhibition of glycosylation. *Eur. J. Cell Biol.* **67,** 285–296
38. Wang, Y., and Rose, B. (1995) Clustering of Cx43 cell-to-cell channels into gap junction plaques: regulation by cAMP and microfilaments. *J. Cell Sci.* **108,** 3501–3508
39. Wang, Y., Mehta, P. P., and Rose, B. (1995) Inhibition of glycosylation induces formation of open connexin-43 cell-to-cell channels and phosphorylation and Triton X-100 insolubility of connexin-43. *J. Biol. Chem.* **270,** 26581–26585
40. Holm, I., Mikhailov, A., Jillson, T., and Rose, B. (1999) Dynamics of gap junctions observed in living cells with connexin43-GFP chimeric protein. *Eur. J. Cell Biol.* **78,** 856–866
41. Solan, J. L., and Lampe, P. D. (2009) in *Connexins: A Guide* (Harris, A., and Locke, D., eds), pp. 263–286, Springer-Verlag New York Inc., New York
42. Maass, K., Ghanem, A., Kim, J. S., Saathoff, M., Urschel, S., Kirfel, G., Grümmer, R., Kretz, M., Lewalter, T., Tiemann, K., Winterhager, E., Herzog, V., and Willecke, K. (2004) Defective epidermal barrier in neonatal mice lacking the C-terminal region of connexin43. *Mol. Biol. Cell* **15,** 4597–4608
43. Simek, J., Churko, J., Shao, Q., and Laird, D. W. (2009) Cx43 has distinct mobility within plasma-membrane domains, indicative of progressive formation of gap-junction plaques. *J. Cell Sci.* **122,** 554–562
44. Duffy, H. S., Iacobas, I., Hotchkiss, K., Hirst-Jensen, B. J., Bosco, A., Dandachi, N., Dermietzel, R., Sorgen, P. L., and Spray, D. C. (2007) The Gap junction protein connexin32 interacts with the Src homology 3/hook domain of Discs large homolog 1. *J. Biol. Chem.* **282,** 9789–9796
45. Stauch, K., Kieken, F., and Sorgen, P. (2012) Characterization of the structure and intermolecular interactions between the connexin 32 carboxyl-terminal domain and the protein partners synapse-associated protein 97 and calmodulin. *J. Biol. Chem.* **287,** 27771–27788
46. Lauf, U., Giepmans, B. N., Lopez, P., Braconnot, S., Chen, S. C., and Falk, M. M. (2002) Dynamic trafficking and delivery of connexons to the plasma membrane and accretion to gap junctions in living cells. *Proc. Natl. Acad. Sci. U.S.A.* **99,** 10446–10451
47. Thomas, T., Jordan, K., Simek, J., Shao, Q., Jedeszko, C., Walton, P., and Laird, D. W. (2005) Mechanisms of Cx43 and Cx26 transport to the plasma membrane and gap junction regeneration. *J. Cell Sci.* **118,** 4451–4462
48. Gaietta, G., Deerinck, T. J., Adams, S. R., Bouwer, J., Tour, O., Laird, D. W., Sosinsky, G. E., Tsien, R. Y., and Ellisman, M. H. (2002) Multicolor and electron microscopic imaging of connexin trafficking. *Science* **296,** 503–507
49. Shaw, R. M., Fay, A. J., Puthenveedu, M. A., von Zastrow, M., Jan, Y. N., and Jan, L. Y. (2007) Microtubule plus-end-tracking proteins target gap junctions directly from the cell interior to adherens junctions. *Cell* **128,** 547–560
50. Bukauskas, F. F., Jordan, K., Bukauskiene, A., Bennett M. V., Lampe, P. D., Laird, D. W., and Verselis, V. (2000) Clustering of connexin 43-enhanced green fluorescent protein gap junction channels and functional coupling in living cells. *Proc. Natl. Acad. Sci. U.S.A.* **97,** 2556–2561
51. Kusumi, A., Fujiwara, T. K., Morone, N., Yoshida KJ, Chadda, R., Xie M, Kasai, R. S., and Suzuki, K. G. (2012) Membrane mechanisms for signal transduction: the coupling of the meso-scale raft domains to membrane-cytoskeleton-induced compartments and dynamic protein complexes. *Semin. Cell Dev. Biol.* **23,** 126–144
52. Sheetz, M. P., Schindler, M., and Koppel, D. E. (1980) Lateral mobility of integral membrane proteins is increased in spherocytic erythrocytes. *Nature* **285,** 510–511
53. Tomishige, M., Sako, Y., and Kusumi, A. (1998) Regulation mechanism of the lateral diffusion of band 3 in erythrocyte membranes by the membrane skeleton. *J. Cell Biol.* **142,** 989–1000
54. Jaqaman, K., Kuwata, H., Touret, N., Collins, R., Trimble, W. S., Danuser, G., and Grinstein, S. (2011) Cytoskeletal control of cd36 diffusion promotes its receptor and signaling function. *Cell* **146,** 593–606
55. Nielsen, P. A., Baruch, A., Shestopalov, V. I., Giepmans, B. N., Dunia, I., Benedetti, E. L., and Kumar, N. M. (2003) Lens Connexins α3Cx46 and α8Cx50 Interact with zonula occludens protein-1 (ZO-1) *Mol. Biol. Cell* **14,** 2470–2481
56. Török, K., Stauffer, K., and Evans, W. H. (1997) Connexin 32 of gap junctions contains two cytoplasmic calmodulin-binding domans. *Biochem. J.* **326,** 479–483
57. Peracchia, C., Sotkis, A., Wang, X. G., Peracchia, L. L., and Persechini, A. (2000) Calmodulin directly gates gap junction channels. *J. Biol. Chem.* **275,** 26220–26224
58. Kojima, T., Kokai, Y., Chiba, H., Yamamoto, M., Mochizuki, Y., and Sawada, N. (2001) Cx32 but not Cx26 is associated with tight junctions in primary cultures of rat hepatocytes. *Exp. Cell Res.* **263,** 193–201
59. Schubert, A. L., Schubert, W., Spray, D. C., and Lisanti, M. P. (2002) Connexin family members target to lipid raft domains and interact with caveolin-1. *Biochemistry* **41,** 5754–5764
60. Kojima, T., Sawada, N., Chiba, H., Kokai, Y., Yamamoto, M., Urban, M., Lee, G. H., Hertzberg, E. L., Mochizuki, Y., and Spray, D. C. (1999) Induction of tight junctions in human connexin 32 (hCx32)-transfected mouse hepatocytes: connexin 32 interacts with occludin. *Biochem. Biophys. Res. Commun.* **266,** 222–229
61. Guerrier, A., Fonlupt, P., Morand, I., Rabilloud, R., Audebet, C., Krutovskikh, V., Gros, D., Rousset, B., and Munari-Silem, Y. (1995) Gap junctions and cell polarity: connexin32 and connexin43 expressed in polarized thyroid epithelial cells assemble into gap junctions, which are located in distinct regions of the lateral plasma membrane domain. *J. Cell Sci.* **108,** 2609–2617
62. Gemel, J., Valiunas, V., Brink, P. R., and Beyer, E. C. (2004) Connexin43 and connexin26 form gap junctions, but not heteromeric channels in coexpressing cells. *J. Cell Sci.* **117,** 2469–2480
63. Sosinsky, G. E., Gaietta G, and Giepmans, B. N. G. (2009) in *Connexins: A Guide* (Harris, A., and Locke, D., eds), pp. 241–262, Springer-Verlag New York Inc., New York
64. Stagg, R. B., and Fletcher, W. H. (1990) The hormone-induced regulation of contact-dependent cell-cell communication by phosphorylation. *Endocr. Rev.* **11,** 302–325
65. Mellman, I., and Nelson, W. J. (2008) Coordinated protein sorting, targeting and distribution in polarized cells. *Nat. Rev. Mol. Cell Biol.* **9,** 833–845
66. Bryant, D. M., and Mostov, K. E. (2008) From cells to organs: building polarized tissue. *Nat. Rev. Mol. Cell Biol.* **9,** 887–901

Downloaded from http://www.jbc.org/ at University of NE Medical Center on December 30, 2015

jbc The Journal of Biological Chemistry
AFFINITY SITES
ASBMB American Society for Biochemistry and Molecular Biology

Cell Biology:

The Carboxyl Tail of Connexin32 Regulates Gap Junction Assembly in Human Prostate and Pancreatic Cancer Cells

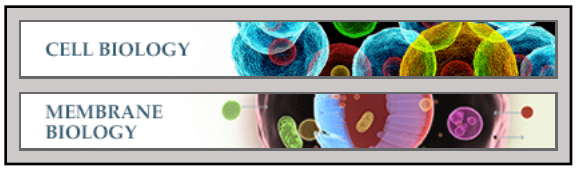

Parul Katoch, Shalini Mitra, Anuttoma Ray, Linda Kelsey, Brett J. Roberts, James K. Wahl III, Keith R. Johnson and Parmender P. Mehta

J. Biol. Chem. 2015, 290:4647-4662.
doi: 10.1074/jbc.M114.586057 originally published online December 29, 2014

Access the most updated version of this article at doi: 10.1074/jbc.M114.586057

Find articles, minireviews, Reflections and Classics on similar topics on the JBC Affinity Sites.

Alerts:
- When this article is cited
- When a correction for this article is posted

Click here to choose from all of JBC's e-mail alerts

Supplemental material:
http://www.jbc.org/content/suppl/2014/12/29/M114.586057.DC1.html

This article cites 63 references, 32 of which can be accessed free at
http://www.jbc.org/content/290/8/4647.full.html#ref-list-1

Downloaded from http://www.jbc.org/ at University of NE Medical Center on December 30, 2015